NAA50 is an enzymatically active Nα-acetyltransferase that is crucial for development and regulation of stress responses

Laura Armbruster, Eric Linster, Jean-Baptiste Boyer, Annika Brünje, Jürgen Eirich, Iwona Stephan, Willy V. Bienvenut, Jonas Weidenhausen, Thierry Meinnel, Ruediger Hell, et al.

Title:

N-terminal acetylation by NatB affects growth and abiotic stress responses in Arabidopsis

Short title: NatB acetylates 20% of the proteome in Arabidopsis

One Sentence Summary: Functional characterization of the plant NatB complex reveals the evolutionary conservation of initiator methionine acetylation and its consequences for adaptation of Arabidopsis to abiotic stresses.

Authors:

Monika Huber[1], Willy V. Bienvenut[2], Eric Linster[1], Iwona Stephan[1], Laura Armbruster[1], Carsten Sticht[3], Dominik Layer[4], Karine Lapouge[4], Thierry Meinnel[2], Irmgard Sinning[4], Carmela Giglione[2,*], Ruediger Hell[1] and Markus Wirtz[1,*]

Authors affiliation:

[1]Centre for Organismal Studies, Heidelberg University, 69120 Heidelberg, Germany. [2]Institute for Integrative Biology of the Cell (I2BC), CEA, CNRS, Université Paris-Sud, Université Paris Saclay, 91198 Gif-sur-Yvette Cedex, [3]Center for Medical Research, Mannheim 68167, Germany. [4]Heidelberg University Biochemistry Center, 69120 Heidelberg, Germany.

***Corresponding authors:**

Markus Wirtz

Phone: +49-6221-54334, Fax: +49-6221-545859

E-mail: markus.wirtz@cos.uni-heidelberg.de

Carmela Giglione

Phone: + 33-169-823597

E-mail: carmela.giglione@i2bc.paris-saclay.fr

Author contributions: MH, EL and ISt identified and characterized the NatB depleted mutants under non-stressed and osmotic stress conditions. CG and TM supervised the N-terminal acetylome profiling. WVB profiled N-termini of the NatB depleted mutants and wild-type. CG, TM and WVB analyzed the N-termini data. CS performed the global transcriptome

analysis. DL and KL expressed, purified and analyzed the *At*NatB complex. IS supervised and planned the biochemical characterization of *At*NatB. LA performed the bioinformatical prediction of NatB substrates based on the substrate specificity elucidated in this paper. MW and RH conceived and directed the study, MW, LA, CG and TM wrote the manuscript with inputs from all authors.

Funding information: Research at Heidelberg was funded by the German Research Council (DFG) via the Collaborative Research Centre 1036 (TP 13 to RH and MW, and TP 22 to IS), and the Leibniz Programme to I.S., and by the European Union by the ERA-CAPS project KatNat to MW and CG. Research in CG lab was supported by ANR Energiome and Sciences-Paris-Saclay. RH and IS are investigators of the Cluster of Excellence:CellNetworks.

Abstract (250 words)

N-terminal acetylation (NTA) is one of the most abundant protein modifications in eukaryotes and is catalyzed in humans by seven N^{α}-acetyltransferases (NatA-F and NatH). Remarkably, the characterization of the plant Nat machinery and its biological relevance is still in its infancy, although NTA has gained recognition as key regulator of crucial processes like protein turnover, protein-protein interaction, and protein targeting.

In this study, we combined *in vitro* assays, reverse genetics, quantitative *N*-terminomics, transcriptomics, and physiological assays to characterize the Arabidopsis NatB complex. We show that the plant NatB catalytic (NAA20) and auxiliary subunit (NAA25) form a stable heterodimeric complex that accepts canonical NatB-type substrates *in vitro*. *In planta*, NatB complex formation was essential for enzymatic activity. Depletion of NatB subunits to 30% of wild-type level in three Arabidopsis T-DNA insertion mutants (*naa20-1*, *naa20-2*, *naa25-1*) decreased growth to 50% of wild-type level. A complementation approach revealed functional conservation between plant and human catalytic NatB subunits, while yeast NAA20 failed to complement *naa20-1*. Quantitative N-terminomics of approximately 1,000 peptides identified 32 *bona fide* substrates of the plant NatB complex. *In vivo*, NatB preferentially acetylated N-termini starting with the initiator methionine followed by acidic amino acids and contributed 20% of the acetylation marks in the detected plant proteome. The global transcriptome and proteome analyses of NatB-depleted mutants suggested a function of NatB in multiple stress responses. Indeed, loss of NatB function increases the sensitivity towards osmotic and high-salt stress. Remarkably, depletion of NatA did not affect these resistances. Hence, NatB but not NatA is required for tolerance in this context.

Introduction

N^{α}-terminal acetylation (NTA) is a global proteome imprinting mechanism conserved in all three domains of life and affecting up to 60% of the soluble yeast proteins and 80-90% of the soluble proteins in *Arabidopsis thaliana* and humans (Polevoda and Sherman, 2003; Falb et al., 2006; Arnesen et al., 2009a; Bienvenut et al., 2012). Despite the prevalent frequency of N-terminal acetylation marks in the proteomes of multi-cellular eukaryotes, the general function of NTA is still discussed controversially. While for individual proteins NTA has been shown to affect folding, aggregation, subcellular localization, degradation, and protein-protein interactions, the overall significance of NTA remains enigmatic (Aksnes et al., 2016).

NTA is catalyzed by N-terminal acetyltransferase (Nat) complexes consisting of at least one catalytic and facultative auxiliary subunits. The auxiliary subunits are in some cases required for catalytic activity and anchor the catalytic subunit to the ribosome (Aksnes et al., 2015a; Aksnes et al., 2019). Since all five yeast Nat complexes, NatA-E, are ribosome-associated and no deacetylases acting on the N-terminus are known, NTA has long been viewed as a static co-translational modification targeting mostly cytosolic proteins (Polevoda et al., 2009; Arnesen, 2011; Giglione et al., 2015). This dogma is challenged by the recent identification of many partially acetylated proteins and post-translational NTA via the Nat complexes NatF-H in multicellular eukaryotes (Linster and Wirtz, 2018; Aksnes et al., 2019).

In humans, the Golgi-associated NatF and the cytosolic NatH control the acetylation of membrane proteins as well as cytoskeleton assembly and cell motility (Drazic et al., 2018). While a NatH homolog is absent in the plant lineage of eukaryotes, a potential homolog of NatF is present in the Arabidopsis genome. The function of the human and plant NatF might differ since the most relevant phenotype of NatF depleted human cells is the disruption of the Golgi-association with the nucleus (Aksnes et al., 2015b), a feature that plant cells are lacking in the first place (Dupree and Sherrier, 1998). NatG is a plant-specific acetyltransferase that localizes to the plastids, where it acetylates N-termini of plastid-encoded as well as imported nuclear-encoded proteins (Dinh et al., 2015). These differences in the post-translationally acting NTA machinery of plants and humans suggest specific adaptations of the NTA in photo-autotrophic eukaryotes and allows for questioning the conservation of the ribosome-associated NTA machinery in eukaryotes.

In a recent study, we demonstrated that the drought stress-related phytohormone abscisic acid (ABA) quickly depleted NatA abundance and thereby altered the plasticity of N-terminal protein acetylation. Remarkably, down-regulation of NatA by genetic engineering resulted in constitutive activation of the ABA response and, consequently, drought-resistant plants (Linster et al., 2015). These findings suggest that NTA in plants is not static but a highly dynamic process, which responds to environmental cues and contributes to the regulation of stress responses. Such active control of NTA has not been observed in other eukaryotes yet and might constitute an adaptation to the sessile lifestyle of plants which forces them to cope with a variety of biotic and abiotic perturbations (Linster and Wirtz, 2018). However, the substrate specificity and the functions of the catalytically active (NAA10) and the ribosome anchor subunit (NAA15) of NatA are conserved between plants and humans (Linster et al., 2015).

NatA acetylates N-termini of nascent polypeptide chains after removal of the initiator methionine (iMet) by methionine aminopeptidases (Frottin et al., 2006). In contrast, NatB recognizes the iMet when it is followed by the acidic amino acids, aspartate or glutamate, or its amidated analogs asparagine and glutamine in yeast and human (Aksnes et al., 2019). Orthologous proteins of the NatB subunits NAA20 (At1g03150) and NAA25 (At5g58450) are encoded in the Arabidopsis genome (Bienvenut et al., 2012; Ferrandez-Ayela et al., 2013), but the substrate specificity of this potential plant NatB complex is unknown. Recently, NatB was shown to accept the plant immune receptor SNC1 (Suppressor of NPR1, Constitutive 1) as a substrate, when the alternative translation of the SNC1 protein usually starting with MMD generates the MD-SNC1 variant. Since NatA recognizes MMD-SNC1, the SNC1 protein is acetylated either by NatA or NatB, which defines SNC1 as an unusual case for substrate recognition by Nat complexes. By controlling the stability of SNC1, NatB contributed in the defense response to the pathogen *Hyaloperonospora arabidopsidis* Noco2, (Xu et al., 2015).

Up to now it was unclear if NatB is also involved in the control of plant abiotic stress responses, and if the substrate specificity and the complex stoichiometry of NatB are conserved in plants.

In this study, biochemical characterization of the potential Arabidopsis NatB subunits NAA20 and NAA25 revealed that they form *in vitro* a stable heterodimeric complex, which accepts canonical NatB-type substrates found in other eukaryotes. We show

that T-DNA insertions in the NatB mutants did not cause full inactivation but depletion of NatB subunits to 30% of wild-type (WT) level. This NatB depletion caused significant retardation of growth, which allows hypothesizing that NatB is indispensable in plants. N-terminal acetylome profiling of the WT and *At*NatB depleted mutants characterized 1,736 total N-termini including 738 unique protein entries. The dataset allowed comparison of the quantification of the acetylation level of 247 unique proteoforms in either genotype with the wild-type. Out of these proteoforms, 70% were substrates of the N-terminal methionine excision (NME) process (514) and 30% (224) did not undergo removal of the first methionine (iMet). The comparison of NTA frequency in WT and NatB depleted plants identified 35 NatB substrates which were most sensitive to depletion of NatB activity and unraveled significant conservation of the NatB substrate specificity in eukaryotes.

Remarkably, NatB-mediated proteome imprinting is essential for the adaptation to salt and osmotic stress in *Arabidopsis thaliana*. The global transcriptome and proteomic analyses of NatB mutants reinforce the role of *At*NatB in cellular stress responses and provide a valuable resource to screen for other metabolic processes affected by NatB depletion in plants.

Result

*At*NAA20 and *At*NAA25 form a stable heterodimeric complex that acetylates NatB-like substrates *in vitro*

While homologs of the two NatB subunits NAA20 and NAA25 have been identified in the Arabidopsis genome (Bienvenut et al., 2012; Ferrandez-Ayela et al., 2013), complex formation and biochemical properties of the candidate plant NatB subunits have not been addressed. To determine the stoichiometry of the *At*NatB complex, *At*NAA25$_{64\text{-}1065}$ and *At*NAA20$_{1\text{-}150}$His$_6$ were co-expressed in insect cells and purified to homogeneity (Supplementary Figure 1), the AtNAA201-150His6 and NAA2564-1065 227 were highly unstable when expressed without their interaction partner. SEC-MALS (size exclusion chromatography coupled to multi-angle light scattering) analysis of the purified proteins revealed that in solution NAA20 and NAA25 form a stable heterodimeric complex (measured M_w= 132.1 ± 0.9 kDa; theoretical M_w= 132.4 kDa, Figure 1A).

Although *At*NAA20 had been recognized as an N-terminal acetyltransferase (Xu et al., 2015), the substrate specificity of free NAA20 and the plant NatB complex remained elusive. To address this aspect, we applied both, *in vitro* and *in vivo* acetylation assays. For the *in vitro* assay, five peptides representing canonical substrates of the major eukaryotic Nats were tested with the purified NatB complex. The known *in vitro* substrates of NatA (SESS, Ree et al. (2015); Weyer et al. (2017)), Naa10/Naa80 (EEEI, Casey et al. (2015); Drazic et al. (2018)) and NatC/E/F (MVNALE and MLGTE, Van Damme et al. (2011)) were not acetylated. *At*NatB was, however, able to acetylate the canonical substrate of human NatB (MDEL, Figure 1B, Starheim et al., (2008)). Therefore, the MDEL peptide was used to determine the enzymatic parameters of the plant NatB complex. The acetyltransferase shows a Michaelis-Menten constant (K_m) of 38.4 ± 9.1 µM for its substrate acetyl-Coenzyme A (acetyl -CoA) and a turnover rate (k_{cat}) of 27.3 ± 1.6 min^{-1}. This is in good agreement with the k_{cat}/K_m value observed for *Candida albicans* NatB (Figure 3C-D, Hong et al. (2017)). Noteworthy, the K_m of NatA (Liszczak et al. (2013); Weyer et al. (2017)), NatB (Hong et al. (2017); this study), and Naa50 (Liszczak et al. (2013)) for acetyl-CoA are all in the range of 24 – 59 µM. In comparison with other enzymes using acetyl-CoA in the cytosol of plant cells (e.g., serine acetyltransferase, K_m = 0.28 mM, (Noji et al., 1998)) the K_m measured for *At*NatB is low, indicating sufficient affinity for acetyl-CoA to trigger efficient catalysis by *At*NatB *in planta*.

Downregulation of NatB activity leads to retarded growth

In order to evaluate the impact of NatB depletion on plant development, we analyzed the T-DNA insertion lines *naa20-1* (SALK_027687) and *naa25-1* (GK-819A05) affected in the catalytic subunit (NAA20) or the auxiliary subunit (NAA25) of *At*NatB. Quantification of the rosette radius over time revealed a slow growth of both mutants in comparison to the WT (Figure 2A, B). After seven weeks, NatB mutants reached approximately three-fourths of the WT size and half of its total rosette fresh weight (Figure 2B, Supplementary Figure 2 and 3). A similar growth retardation was observed in the NatB T-DNA insertion line *naa20-2* (SAIL_323_B05), which had previously been characterized by Ferrandez-Ayela et al. (2013) (Supplementary Figure 2E). Since Ferrández-Ayela and colleagues had reported defects in embryo development of *naa20-2,* we quantified viable pollen and seeds per silique in the *naa20-1* and *naa25-1* mutants. No significant differences in comparison to WT plants were detected when plants were grown under short day conditions and optimal

nutrient supply (Supplementary Figure 4). This discrepancy might be explained by the different growth conditions used in both studies.

We quantified the impact of the T-DNA insertion in the *NAA20* and *NAA25* genes on the expression of NatB subunits by analyzing the abundance of *NAA20* and *NAA25* transcripts via qRT-PCR. In both, *naa20-1* and *naa25-1* lines, remaining *NAA20* or *NAA25* transcripts could be detected (Figure 2C, D). In addition, the translation of the *NAA25* transcript was verified with a specific antiserum, confirming that *naa25* mutants retain 30% of the WT NAA25 protein level (Figure 2E, F). These findings demonstrate that *naa20-1* and *naa25-1* are not loss-of-NatB function mutants, but were significantly depleted in NatB abundance.

The human NAA20 homologue can functionally complement the Arabidopsis *naa20* mutant

To verify whether the T-DNA insertion in the *NAA20* gene was causative for the *naa20-1* phenotype, the mutant was complemented with a construct expressing the endogenous Arabidopsis NAA20 protein (*At*NAA20) under the control of the constitutive CaMV 35S promoter. The successful transformation was confirmed by PCR-based genotyping (Supplementary Figure 5A). The resulting complemented *naa20-1* mutants had a WT-like habitus and a relative rosette dry weight indistinguishable from the WT control (Figure 3A, -C). When expressed via the same construct, the human NAA20 orthologue (*Hs*NAA20) was able to rescue the Arabidopsis *naa20-1* phenotype as well (Figure 3A, 3C, Supplementary Figure 5B). Remarkably, expression of the yeast NAA20 protein (*Sc*NAA20) using the same promoter, ribosome binding site and terminator failed to complement the *naa20-1*, although the *ScNAA20* transcript was produced as shown by semi-quantitative RT-PCR (Figure 3B, C, Supplementary Figure 5C, -D, Supplementary Figure 6). This observation is in agreement with the complementation of yeast *natB* loss-of-function mutants by simultaneous expression of both human NatB subunits, but not of its single subunits in the respective *naa20* or *naa25* single knockouts (Van Damme et al., 2012). Our results suggest that endogenous *At*NAA25 assembles with *AtNAA20* or *Hs*NAA20 to a functional NatB complex, while interaction with *Sc*NAA20 either failed or produced a catalytically inactive complex *in planta*. Furthermore, one cannot exclude that, unlike the *Hs*NAA20, the *Sc*NAA20 might display a different specificity with respect to some plant substrates. The relevance of species-specific differences

for complementation of plant loss-of-function mutants has already been evidenced in the case of another N-terminal modifying enzyme, N-Myristoyltransferase (Pierre et al., 2007).

Bioinformatical screen for potential NatB substrates

The functional conservation between the human and the Arabidopsis NAA20 protein suggests that the substrate specificity of the NatB complex might also be evolutionary conserved. Thus, we screened the Arabidopsis proteome for potential NatB targets based on the database of known-classical NatB substrate specificity (ME, MD, MN, MQ). This search revealed 11,399 nuclear-encoded Arabidopsis protein variants starting with a canonical plant NatB substrate N-terminus (23.6% of the total proteome, Supplementary Table 1). For 4,927 potential NatB substrates the subcellular prediction was inconclusive according to TAIR10-Subcellular Predictions (Kaundal et al., 2010). Out of the remaining 6,472 proteins with well predicted subcellular localizations, 1,010 proteins are supposed to be translated at the rough ER due to their extracellular localization (472) or localization in the Golgi body (60) or the cell membrane (478) (Reid and Nicchitta, 2015). 5,462 protein variants are predominantly translated by cytoplasmic ribosomes, and stay in the cytoplasm (969, 17.7%) or are translocated to the nucleus (3,372, 61.7%), the mitochondria (589, 10.7%) or the plastids (532, 9.7%). At least these 5,462 proteins translated by cytoplasmic ribosomes are prime candidates for proteome imprinting by NatB since eukaryotic NatB is associated with cytoplasmic polyribosomes (Polevoda et al., 2008).

The Arabidopsis NatB complex targets the iMet of protein N-termini

To verify the *in vivo* substrate specificity of *At*NatB, we examined the N-terminomes of cytosolic soluble proteins from leaves of the WT, and the NatB depleted plants (*naa20-1* and *naa25-1*) by the 'Stable Isotope Labelling Protein N-terminal Acetylation Quantification' method (SILProNAQ, Bienvenut et al. (2017a)). Experimental data were then processed with the EnCOUNTer tool (Bienvenut et al., 2017b) to provide an accurate measurement of the N-terminal acetylation pattern and frequency in WT and NatB depleted plants. Analysis of these three genotypes together identified 1,736 N-termini corresponding to 738 non-redundant proteoforms

(Supplementary Table 2). The analysis of these unique proteoforms unraveled that 514 (70%) underwent removal of iMet following the N-terminal methionine excision rule (Frottin et al., 2006), whereas 224 proteoforms (30%) still displayed their iMet. 94% of the iMet starting N-termini had at position two an amino acid with a large lateral chain (Supplementary Table 2).

Among all identified proteoforms we were able to quantify according to criteria defined in Bienvenut et al., (2017b) 436 unique N-termini (271 in the WT, 360 in *naa20-1* and 339 in *naa25-1* mutant backgrounds). Among the quantified N-termini in these three genotypes, 333 underwent removal of iMet (76%) and 103 (24%) retained their iMet. In the WT, 87% (55/67) of the quantified N-termini that retained the iMet, were fully acetylated (acetylation yield >95%), while 13% (12/67) were partially or not acetylated (Figure 4A, Table 1). The fully acetylated proteins are predominantly classical NatB-substrates (N-termini featuring iMet followed by Glu>Asp>>Asn, (48/55). Only two NatB-type N-termini were found in the groups of partly or non-acetylated proteins (2/12). The groups of weakly or non-acetylated proteins consisted mostly of iMet-Lys N-termini (7/12), together with three putative NatC-type N-termini (iMet-Ile and iMet-Leu, 3/12).

The SILProNAQ approach revealed a 25% decrease in the overall N-acetylation level in NatB depleted plants (*naa20-1* and *naa25-1*) when compared to WT (Figure 4A). The acetylation frequency of N-termini devoid of the iMet was unaffected in NatB depleted mutants (Figure 4B), which is in agreement with the acceptance of these N-termini as substrates by NatA (Linster et al., 2015). Remarkably, all N-termini with decreased acetylation retained their iMet (Figure 4C). We identified 32 proteins that were fully acetylated in the WT and displayed significantly less NTA in NatB depleted mutants (Table 2). Those proteins predominantly displayed the acidic amino acids Asp and Glu and to a minor extent Asn at position two (Figure 4E and Table 1). This set of *in planta*-detected NatB substrates independently confirms the substrate specificity determined with the *in vitro* reconstituted plant NatB and are, thus, defined as *bona fide* substrates in the here analyesd subset of the proteome (Figure 1). Furthermore, three partly acetylated proteins in the WT showed lowered acetylation in NatB depleted plants. The N-terminus of the indole-3-butyric acid response 1 protein (starting with iMet-Asp, AT4G05530.1) was 80% acetylated in the WT but found to be not acetylated in NatB depleted plants (NTA level: <1%). The two

remaining proteins (HMGB2 and HMGB3) had Lys at position two, and their N-termini were less than 16% acetylated in the WT. In the NatB depleted mutants, the NTA levels of both proteins were decreased to 8-13%.

In addition to the 35 proteins that were less acetylated in NatB depleted plants, we observed eight in the WT fully acetylated proteoforms that could not be quantified in NatB depleted plants but were experimentally characterized without NTA modification (Supplementary Table 2). This set of potential NatB proteins included the salt stress-related protein AT1G13930 (see below). In accordance with the here deteremined *At*NatB susbstrate specificity these proteins also possess Glu>Asp>Asn as second residues.

After characterization of the *in vivo* substrate specificity of the plant NatB we rechecked the number of NatB substrate N-termini in the WT protein fraction and detected 499 N-terminal peptides of which 149 started with an iMet. Out of the iMet retaining peptides, 108 displayed an N-terminus starting with iMetAsp, iMetGlu, or iMetAsn (Supplementary Table 3), which can be accepted by the plant NatB according to the here performed *in vitro* and *in vivo* analysis of the AtNatB substrate specificity (Figure 1 and Figure 4). This analysis defines 22% of the detected N-termini in the leaves of the WT as substrates of NatB. Due to the remaining NatB activity (approx. 30% of WT level) in the *naa20-1* or *naa25-1* mutants not all of these substrates were less acetylated in the mutants. Notably, the majority of potential NatB substrates were found to be fully acetylated in the WT leaf under non-stressed conditions. In agreement with the finding that approx. 22% of the detected N-termini from soluble proteins match the substrate specificity of NatB, a significant increase of free N-termini in NatB-depleted mutants was demonstrated by fluorescent labeling of free protein N-termini with NBT-Cl (Figure 4D).

In parallel to the SILProNAQ analysis, a 2D gel approach was applied to identify further NatB substrates. Total protein extracts from WT or *naa20-1* plants were separated by 2D-gel electrophoresis according to their size and charge. If a basic shift was observed for a protein species, this was attributed to the increased positive charge of the protein due to loss of NTA. The 2D gel analysis yielded three reproducible shifts (Figure 4F and Supplementary Figure 7). In the case of the salt stress-related protein AT1G13930, we could verify that the N-terminal peptide (iMet-Asn) of the acidic proteoform was acetylated in both genotypes whereas the basic

proteoform was unacetylated. These results demonstrate lowered NTA of AT1G13930 in *naa20-1* when compared to wild type and, independently confirm the identification of AT1G13930 as a NatB substrate by the SILProNAQ approach. The SILProNAQ approach also supports the lowered NTA of nucleoside diphosphate kinase 1 (AT4G09320, Table 2), which was identified in spot 2 and spot 2* within the 2D gel approach (Figure 4F).

NatB depletion results in sensitivity to high salt and osmotic stress

Based on the results above and the identification of the salt sensitivity modulator AT1G13930 as a NatB substrate (Figure 4F), we analyzed the performance of NatB depleted mutants under high salt and osmotic stress. To this end, seeds were germinated on 1xMS medium supplemented with either 100 mM NaCl, 3 % mannitol or no osmoticum, respectively. Both NatB depleted mutants showed a significant reduction in germination efficiency when grown on NaCl or mannitol, demonstrating that NatB is essential for efficient germination under hyperosmotic or high salt conditions (Figure 5A, -C). To prove that this diminished germination efficiency was exclusive to NatB mutants rather than a pleiotropic side effect of impaired NTA at the ribosome, the NatA depleted lines *amiNAA10* and *amiNAA15* were subjected to the same stress. Depletion of NatA activity did not influence the germination rate under hyperosmotic or high salt conditions (Figure 5B, -D), indicating a specific function of NatB mediated proteome imprinting during these stresses. To assess the effect of osmotic stress on adult plants, wild-type and *naa20-1* mutants were grown on ½ x MS medium supplemented with 1 % sucrose for two-weeks under short-day conditions. Subsequently, the plants were transferred to the same medium (control) or medium supplemented with 150 mM NaCl. After two weeks, the growth of the primary root was evaluated. Although both plants experienced salt stress as indicated by the increased transcription of the salt stress marker gene *HB-7*, only *naa20-1* mutants displayed a significantly impaired primary root growth upon high salt medium (Supplementary Figure 8).

Global transcriptome analysis of *naa20* depleted mutants

Based on the vast number of predicted NatB substrates, NatB depletion was expected to affect a variety of cellular processes. A global analysis of the leaf transcriptome revealed differential regulation (>1.5-fold up- or downregulated) of 494

transcripts (~ 2 % of all tested transcripts) when comparing six-week-old soil grown *naa20-1* mutants to wild-type plants (Gene Expression Omnibus record: GSE132978). In this context, 322 transcripts were downregulated and 172 transcripts upregulated (Supplementary Table 4). To identify putatively NatB-affected biological processes, we performed a gene ontology enrichment analysis for differentially regulated genes in *naa20-1* using the DAVID Bioinformatic Resources tool v. 6.8 (Table 3, Supplementary Table 5). Among the upregulated transcripts, genes involved in transition metal transport, namely zinc ion transport, and lipid localization were significantly (3-fold enrichment, $p<0.05$) enriched. Among the downregulated transcripts, however, genes mediating plant stress responses were considerably overrepresented. The downregulated responses to environmental perturbations included not only the reaction to light intensity or toxins but also distinct steps within the immune response, e.g., responses to bacteria, fungi, viruses, wounding and reactive oxygen species. Taken together, this pattern of transcriptional regulation in NatB-depleted mutants suggest an even broader function of NatB in the plant immune response than previously shown by Xu et al. (2015).

Discussion

The Arabidopsis NatB complex is involved in a variety of developmental processes, including leaf shape formation and transition from vegetative to generative growth. The developmental defects observed in NatB mutants had previously been attributed to a total loss-of-NatB activity (Ferrandez-Ayela et al., 2013). Here, we demonstrate that the available NatB T-DNA insertion lines retain a diminished NatB expression and hence do not constitute full knockouts. This finding not only demonstrates the importance of functional NatB-mediated imprinting of the proteome with acetylation marks but also raises the question towards the severity of the total loss-of-NatB activity. Since full-loss-of NatB function mutants by T-DNA insertion are currently unavailable, this question should be addressed by CRISP-Cas9 mediated gene-disruption in future studies. Loss of NatA causes abortion of the plant embryo at the globular stage (Linster et al., 2015). It is tempting to speculate that loss of NatB might as well be lethal in plants. Remarkably, depletion of NatB activity in human cells impairs cellular proliferation and affects tumorigenesis (Ametzazurra et al., 2008; Starheim et al., 2008; Ametzazurra et al., 2009). In yeast, NatB is dispensible like loss of any other Nat complex. The yeast *natB* mutants showed the most severe

phenotypes when compared to *natA*, *natC*, *natD* or *natE* mutants. These phenotypes included cytoskeleton defects, cell cycle arrest, and severe growth retardation (Polevoda et al., 2003; Singer and Shaw, 2003).

NatB substrate specificity is conserved in yeast, humans and plants

Except for the NatA complex, the substrate specificity of plant Nats was barely investigated in previous works (Pesaresi et al., 2003; Linster et al., 2015). This lack of knowledge prompted us to determine the NatB substrate specificity by N-terminal acetylome profiling of NatB depleted mutants and by analyzing the enzymatic activity of reconstituted *At*NatB *in vitro*. Biochemical characterization of the heterodimeric plant NatB and the proteomic approach revealed the clear preference of NatB towards N-termini retaining their iMet followed by glutamate or aspartate. To a minor extent also iMet followed by asparagine were accepted as substrate in the here analysed subset of the leaf proteome. The recognition of those substrates recapitulates the established substrate specificity of yeast and human NatB (Helbig et al., 2010; Van Damme et al., 2012), and suggests significant conservation of the NatB substrate specificity in fungi, animals, and plants. Despite the conserved substrate specificity of eukaryotic NatB complexes, only *Hs*NAA20 but not *Sc*NAA20 was able to complement the retarded growth phenotype of the *naa20-1* plants. A similar observation was reported for NatA: Yeast loss-of-NatA mutants are rescued by reconstituted human NatA complex, whereas the human catalytic or auxiliary NatA subunits alone cannot complement the respective single loss-of-function mutants, suggesting significant structural subunit differences between the species (Arnesen et al., 2009b). Similarly, significant differences in the complex assembly have been reported for *At*NatC and *Sc*NatC (Pesaresi et al., 2003).

The here determined substrate specificity of the plant NatB suggests that ~24 % of the plant proteome is imprinted by NatB (bioinformatical prediction). In agreement with such a high number of NatB substrates, 21% of the proteins whose N-terminus could be quantified in wild-type and NatB mutants were identified as substrates of NatB. Such broad substrate recognition has also been determined for NatB of other eukaryotes (Helbig et al., 2010; Van Damme et al., 2012), and can be explained by the predominant interaction of the first two amino acids of the substrate peptide with the active site of the catalytic NatB subunit (Hong et al., 2017). Furthermore, depletion of *At*NatB to 30% of wild-type level in *naa20-1* and *naa25-1* caused more

than 1.5-fold increase of total free N-termini (Figure 4). Since the NatB depleted mutants retain 30% of the wild-type NatB activity, we could only identify 35 substrates to be unambiguously less acetylated in *naa20-1* and *naa25-1* mutants. Thus, these 35 proteins represent the apparently most sensitive substrates of *At*NatB in leaves.

The proteins encoded by AT5G10780 and AT1G64520 carry the amino acid aspartate as penultimate residue and are both 99% acetylated in wild-type plants. Remarkably, the knockdown of NatB in *naa20* or *naa25* mutants reduced the acetylation yield for AT1G64520 to 2 %, whereas the protein encoded by AT5G10780 remained acetylated to 87-88 % in the mutant. Thus the substrate specificity and degree of acetylation by NatB predominantly depends on the first two amino acids but is also shaped by additional primary sequence information or the secondary structure of the nascent chain. In this respect, a recent study demonstrates that alpha-helices could fold co-translationally within the ribosomal exit tunnel (Nilsson et al., 2015), which may interfere with binding into the catalytic pocket of NAA20.

Acetylation via different Nats regulates specific plant stress responses

Unlike NatA, which had previously been shown to mediate the drought stress response in *Arabidopsis thaliana*, NatB had so far never been associated with any plant abiotic stress response. The vast number of potential NatB substrates and the overall decrease of stress-responses at the transcriptional level in *naa20-1* mutants prompted us to analyze the performance of NatB depleted mutants upon protein-harming stress. We selected high salt and osmotic stress because both cause misfolding of proteins and consequently affects proteostasis (Chen et al., 2019). Indeed, the plant NatB mutants were sensitive to osmotic stress which has also been shown for yeast NatB mutants (Van Damme et al., 2012). A protective role of *Sc*NAA20 dependent acetylation with respect to protein degradation and susceptibility to specific stresses has been suggested (Nguyen et al., 2019). Notably, the depletion of NatA activity did not lead to hypersensitivity against osmotic or high salt stress in plants, although NatA targets approximately twice as many substrates as NatB (Linster and Wirtz, 2018). Vice versa, the knockdown of NatA results in drought-tolerant plants, while NAA20 depleted plants were drought sensitive as the wild-type (Linster et al., 2015). Despite the high number of substrates acetylated by

each Nat complex, our results support discrete functions of Nat complexes during specific stresses.

In human and yeast, proteomics and transcriptome analysis of NatB depleted cells show that NatB substrates are mainly involved in DNA processing and cell cycle progression (Caesar and Blomberg, 2004; Caesar et al., 2006; Ametzazurra et al., 2008). The global transcriptome analysis of *naa20* mutants relates acetylation via NatB in plants to transition metal transport, lipid localization, and stress responses. One particular stress response of interest is the defense against pathogens. Among the transcripts downregulated in *naa20* mutants, transcripts implicated in the defense against pathogens are significantly enriched, which might translate into a weaker response to biotic stresses in NatB depleted plants. Indeed, a connection between Nat-mediated protein stability and pathogen resistance was recently shown by Xu et al. (2015). Xu and colleagues found that in Arabidopsis a depletion of NatB subunits caused decreased immunity against the virulent oomycete *Hyaloperonospora arabidopsidis* Noco2 mediated by destabilization of the plant immune receptor SNC1 (Suppressor of NPR1, Constitutive 1). Interestingly, the stability of SNC1 is antagonistically regulated by NatB and NatA. While acetylation of the receptor via NatA serves as a degradation signal, acetylation via NatB stabilizes SNC1 (Xu et al., 2015).

Conclusion

NTA by the NatB complex has been well characterized in yeast and humans, the role of NatB in phototrophic organisms was less clear. The combination of biochemical and reverse genetic approaches elucidate the substrate specificity and stoichiometry of subunits in the Arabidopsis NatB complex and reveal the global transcriptional consequences of NatB downregulation. The here applied high salt and osmotic stress-experiments uncover a specific role of the *At*NatB complex under a physiologically relevant abiotic stress. These findings expand the view on NatB function beyond its influence on plant development. In combination with our previous findings on the role of NatA in the plant drought stress response, these results allow speculating that dynamic regulation of N-terminal protein acetylation modulates plant stress responses and that distinct Nat complexes have specific roles in this modulation.

Materials and Methods

Plant material and growth conditions

All work was performed with *Arabidopsis thaliana* ecotype Columbia-0 (Col-0). The utilized T-DNA insertion lines *naa20-1* (SALK_027687, successfully selected on kanamycin), *naa20-2* (SAIL_323_B05, successfully selected on glufosinate) and *naa25-1* (GK-819A05, not selected on sulfadiazine in this study) originate from the SALK, SAIL and GABI-KAT collections (Sessions et al., 2002; Alonso et al., 2003; Rosso et al., 2003). The NatA artificial microRNA (amiRNA) knock-down lines, *amiNAA10* and *amiNAA15*, were created by Linster et al. (2015). All experiments except the osmotic stress treatment (described below) were conducted with plants grown on medium containing one half soil and one half substrate 2 (Klasmann-Deilmann, Germany) under short day conditions (8.5 h light, 100 µE light photon flux density, 24 °C at day, 18 °C at night and 50 % humidity).

Osmotic stress treatment

To analyze the implications of NatB-mediated N-terminal acetylation under osmotic stress, seeds of NatB depleted mutants were surface-sterilized with 70 % ethanol (5 min) and 6 % NaClO (2 min) followed by three washing steps with sterile water. After two days of stratification at 4 °C, seeds were germinated under short day conditions on 1x Murashige & Skoog (MS) medium (4 g/l MS-salts (Duchefa, Netherlands), 1 % (w/v) sucrose, 0.4 g/l MES, 0.7 % (w/v) micro agar, pH 5.9). To induce osmotic stress, plates were supplemented with either 100 mM NaCl or 3 % mannitol.

To assess the effect of osmotic stress on adult plants, seeds of wild-type and *naa20-1* mutants were surface sterilized and stratified as described above. The plants were grown on ½ x MS medium supplemented with 1 % sucrose for two-weeks under short-day conditions. Subsequently, the plants were transferred to the same medium (control) or medium supplemented with 150 mM NaCl. After two weeks, the growth of the primary root was evaluated. The transcript levels of the salt stress marker *HB-7* (AT2G46680, Liu et al., 2007) and the putative NatB substrate salt stress-related protein (AT1G13930) were assessed via quantitative real-time PCR (see below).

PCR

PCR for identification of T-DNA insertion lines was performed with the Taq-DNA Polymerase (New England Biolabs, M0267L). Genotyping of T-DNA insertion lines *naa20-1, naa20-2* and *naa25* was conducted with specific primer combinations for the wild-type (NAA20_LP, NAA20_RP, NAA25_LP and NAA25_RP) and mutant

allele (SALK_BP and GK_BP). For cloning, DNA was amplified with the high-fidelity DNA polymerase Phusion (New England Biolabs, M0530L). All enzymes were used according to the supplier's instructions manual. The corresponding primer sequences are listed in the Supplementary Table 6.

Quantitative real-time PCR

To analyze Nat transcript levels, total RNA was extracted from leaves using the RNeasy Plant Kit (Qiagen, Germany). Subsequently, total RNA was transcribed into complementary DNA (cDNA) with the RevertAid H Minus First Strand cDNA Synthesis Kit using oligo(dT) primers (Thermo Scientific). All reactions were conducted according to the supplier's protocol. The cDNA was analyzed by qRT-PCR with the qPCRBIO SyGreen Mix Lo-ROX (PCR Biosystems) and TIP41 (AT4G34270, Czechowski et al. (2005)) as reference gene. The primer sequences for specific amplification of genes are listed in the Supplementary Table 6. Data was analyzed via Rotor-Gene Q Series Software (v2.0.2).

Stable transformation of *Arabidopsis thaliana*

To analyze the conservation between NAA20 orthologues, the Arabidopsis *naa20-1* line was transformed with the endogenous, as well as the human and yeast NAA20 sequences. The genes of interest were amplified via PCR using Gateway compatible primers (*At*NAA20-N, *At*NAA20-C, *Hs*NAA20-N, *Hs*NAA20-C, *Sc*NAA20-N and *Sc*NAA20-C, see Supplementary table 6). The NAA20 sequences were then cloned into the binary vector pB2GW7, where they were expressed under the control of the CaMV 35S promoter. Stable transformation was conducted according to the floral dip method for Agrobacterium-mediated transformation of *Arabidopsis thaliana* described by Clough and Bent (1998). Transformants were selected using 200 mg/l BASTA at the age of two weeks. The presence of stably transformed constructs was confirmed using primers either amplifying the BASTA (BASTA_fw and BASTA_rev) or the ScNAA20 (*Sc*Nat3_fw and *Sc*Nat3_rev) sequence. To control the expression of the ScNAA20 construct, semi-quantitative RT-PCR was performed via Taq-DNA Polymerase using the housekeeping gene actin as a positive control (*Sc*NAA20_fwd, *Sc*NAA20_rev, Actin_fwd and Actin_rev).

Generation of a NAA25 specific antibody

The DNA sequence encoding the amino acids 233-430 of NAA25 was PCR amplified with primers comprising restriction sites for NcoI and HindIII (NAA25_fwd and

NAA25-rev, Supplementary Table 6) and cloned into pET20b (C-terminal His-fusion) using the newly introduced restriction sites. Correct cloning was verified by DNA sequencing. For protein expression, the vector was transformed into *E. coli Rosetta DE3 pLysS* (Novagen) by electroporation. Cell cultures were grown in 300 ml selective LB medium at 37 °C and protein expression was induced at an OD_{600} of 0.8 with 1 mM IPTG (isopropyl-β-D-thiogalactoside). After 5 h of incubation, the cells were harvested by centrifugation and stored at -80 °C until further usage. *E. coli* pellets containing recombinant proteins were lysed by sonication in 5 ml resuspension buffer (250 mM NaCl, 50 mM Tris pH 8,0 supplemented with 0.5 mM PMSF). The crude extract was centrifuged and the resulting pellet was dissolved in 10 ml denaturation buffer (8 M urea, 10 mM NaH_2PO_4, 1 mM Tris, pH 8.0) using the Ultra-Turrax® T25. The protein fraction was cleared by centrifugation (10 min at 17,000 rpm, 4 °C). The supernatant was used for further separation via SDS-PAGE. The NAA25 fragment band was cut out and the protein was eluted in denaturation buffer using the electro elution chamber Biotrap BT 1000 (Schleicher and Schuell) according the manufacturer`s instructions. The denatured protein fraction was concentrated using the Vivaspin® 2 Centrifugal Concentrator (10.000 MWCO PES) and used for the immunization of rabbits.

Protein extraction from Arabidopsis leaf tissue

Total soluble protein extracts were isolated from 200 mg ground leaf material using 500 µl pre-cooled extraction buffer (50 mM HEPES pH 7.4, 10 mM KCl, 1 mM EDTA, 1 mM EGTA, 10 % v/v glycerol) supplemented with 10 mM DTT and 0.5 mM PMSF. Protein extracts were cleared by centrifugation (10 min at 13,000 rpm, 4 °C) and the protein concentration was quantified according to Bradford (1976).

SDS–PAGE and immunological detection

Protein extracts were subjected to SDS-PAGE according to Laemmli (1970) and blotted to a PVDF membrane using Mini-ProteanTM II cells (BioRad). The primary NAA25 antibody and the secondary horseradish peroxidase-linked anti-rabbit antibody (#AS10 852, Agrisera) were diluted 1: 5,000 and 1: 25,000 in 1x TBS-T (50 mM Tris pH 7.6, 150 mM NaCl, 0.05 % Tween-20) supplemented with 0.5 % BSA. Membranes were developed using the SuperSignal West Dura Extended Duration Substrate (Thermo Scientific) according to the manufacturer's instructions. The resulting signals were recorded using the ImageQuant LAS 4,000 (GE

Healthcare) and subsequently quantified with the ImageQuant TL Software (GE Healthcare).

Separation of total Arabidopsis protein by two-dimensional PAGE

To identify putative NatB substrates, 200 mg leaf material of nine-week-old, soil grown wild-type and *naa20* plants was ground in liquid nitrogen. Proteins were precipitated with trichloric acid/acetone. Subsequently, 160 mg protein of protein were subjected to isolectric focusing followed by SDS-PAGE as described in Heeg et al., 2008. The separated proteins were visualized by silver staining (Blum et al., 1987). Putative substrates were identified with MALDI-TOF-MS analysis as outlined in Heeg et al., 2008.

Determination of the global transcriptome

The peqGOLD Total RNA Kit (Peqlab) was used to extract RNA from 17-day-old wild-type and *naa20-1* seedlings grown on 1xMS medium under short day conditions. A global transcriptome analysis was performed using the Affimetrix (High Wycombe, UK) *Arabidopsis thaliana* Genechip (AraGene-1_0st-typ) as described in detail by Linster et al., 2015. Transcripts which were differentially regulated (>1.5-fold up- or downregulated, $p<0.05$) in *naa20-1* compared to wild-type were functionally annotated. Overrepresented biological processes were identified based on the DAVID Bioinformatics Resources 6.8 gene ontology analysis (Huang da et al., 2009b, a).

Quantification of N-terminal protein acetylation

Soluble leaf proteins from six-week-old soil-grown wild-type and the NatB depleted mutants, *naa20-1* and *naa25-1*, were extracted for quantification of N-terminal protein acetylation. The extracted proteins were processed and enriched by an SCX approach for quantification of N-terminal peptides using mass spectrometry as described in Linster et al., (2015).

Determination of free N-termini

To determine the relative amount of free N-termini in wild-type, *naa20-1* and *naa25-1* plants, soluble proteins were extracted from leaf material (50 mM sodium citrate buffer pH 7.0, 1 mM EDTA). For removal of free amino acids, protein extracts were subsequently gel filtrated via PDMiniTrap G-25 columns (GE Healthcare). The

labeling of free N-termini was performed with 2.5 µM extracted protein and 0.5 mM NBD-Cl (Bernal-Perez et al., 2012) in 50 mM sodium citrate buffer pH 7.0 supplemented with 1 mM EDTA. After 14 h of incubation at room temperature, the fluorescence intensity was quantified via a FLUOstar Omega plate reader (BMG Labtech; excitation: 470±10; emission: 520 nm).

Construction of *At*NatB Baculovirus

*At*NAA25$_{64\text{-}1065}$ and *At*NAA20$_{1\text{-}150}$ coding sequences were amplified by PCR from *Arabidopsis thaliana* cDNA and a C-terminal His-tag was introduced into the *At*NAA20 sequence (Supplementary Table 1). The PCR products were cloned into pET24d and pET21d (Novagen), respectively. *At*NAA25$_{64\text{-}1065}$ and *At*NAA20$_{1\text{-}150}$His$_6$ coding sequences were subcloned from the pET vectors into a pFastBacDUAL vector (Invitrogen). A bacmid was generated by transferring the plasmid into electrocompetent DH10 MultiBac *E. coli* cells (Geneva Biotech). Afterwards, the Escort IV Transfection reactant (Sigma) was used to transfect *Spodoptera frugiperda* (Sf9) cells, cultured in SFM II medium supplemented with 5% EX-CELL TiterHigh (Sigma) and appropriate antibiotics, with the obtained bacmid DNA. Finally, the baculovirus was amplified twice before using it for protein expression.

Protein purification

Sf9 insect cells were grown in SFM II medium supplemented with 5 % EX-CELL TiterHigh (Sigma) and appropriate antibiotics to a density of 8x10^5 cells/ml. 250 ml of cultures were infected using the *At*NAA25$_{64\text{-}1065}$ *At*NAA20$_{1\text{-}150}$His$_6$ baculovirus. The cells were grown at 27 °C and harvested after 3 days by centrifugation (15 min, 1500 g and 4 °C). For purification, the harvested cells were resuspended in lysis buffer (20 mM HEPES pH 7.5, 500 mM NaCl, 20 mM $MgCl_2$, 20 mM KCl, 20 mM Imidazole, supplemented with protease inhibitor mix and benzonase) and lysed using a microfluidizer (M-110L, Microfluidics). The lysate was cleared by ultra-centrifugation (50000 g, 30 min, 4 °C) and the supernatant was loaded on Ni-NTA beads (Qiagen). The *At*NAA25$_{64\text{-}1065}$ *At*NAA20$_{1\text{-}150}$His$_6$ complex was eluted using lysis buffer supplemented with 250 mM imidazole and loaded on a Superdex 200 16/60 gel-filtration column (GE Healthcare) equilibrated in gel-filtration buffer (20 mM HEPES pH 7.5, 500 mM NaCl) for size exclusion chromatography.

Multi-angle light scattering (MALS)

0.1 mg *At*NAA25$_{64-1065}$ *At*NAA20$_{1-150}$His$_6$ was injected onto a Superdex 200 10/300 gel-filtration column (GE Healthcare) in gel-filtration buffer. The column was connected to a MALS system (Dawn Heleos II 8+ and Optilab T-rEX, Wyatt Technology). Measurements were performed in triplicates and data was analyzed using the Astra 6 software (Wyatt Technology).

In vitro acetyltransferase assays

Acetylation activity of *At*NAA25$_{64-1065}$ *At*NAA20$_{1-150}$His$_6$ was recorded using a SpectraMax M5e MultiMode Microplate reader by continuously detecting the absorbance at 412 nm. The assays were performed at 25 °C with 1.0 mM MDEL peptide (PLS GmbH) mixed with Acetyl CoA (12.5-500 µM) in reaction buffer (2 mM 5,5´dithiobis(2-nitrobenzoic acid), 70 mM HEPES pH 7.5, 70 mM NaCl, 20 mM sodium phosphate dibasic pH 6.8, 2 mM EDTA). Then the enzyme (final concentration 500 nM) was added to start the reaction. To determine the substrate specificity of *At*NatB, various peptides (SESS, EEEI, MDEL, MVNALE and MLGTE (all PLS GmbH) and a constant AcCoA concentration of 100 µM were used. The concentration of the produced CoA was quantified after 30 min. Control reactions were performed in the absence of the peptides. Measurements were taken in triplicates.

Basic statistical analysis

Statistical analysis was conducted using SigmaPlot 12.0. Means from different sets of data were analysed for statistically significant differences with the Holm-Sidak One-Way ANOVA test or the student's t-test. Significant differences ($P<0.05$) are indicated with different letters.

691 **Tables**

692

693 **Table 1: List of all protein N-termini without methionine excision identified and**
694 **quantified in wild-type.** Full acetylation is defined as an N-terminal acetylation rate
695 higher than 90 %, while no acetylation refers to an acetylation rate lower than 10 %.
696 Partially acetylated proteins range between these values.

Entry	Description	N-terminus	% NTA WT
AT5G10780.1	ER membrane protein complex subunit-like protein	MDKGKAVMGT	100
AT1G06210.1	ENTH/VHS/GAT family protein	MDKLKIAEWG	100
AT1G18070.1	Translation elongation factor EF1A/initiation factor IF2g family protein	MDLEAEIRAL	100
AT3G12800.1	short-chain dehydrogenase-reductase B	MDSPFKPDVV	100
AT2G13360.1	alanine:glyoxylate aminotransferase	MDYMYGPGRH	100
AT2G23120.1	Late embryogenesis abundant protein, group 6	MEAGKTPPTT	100
AT2G21620.1	Adenine nucleotide alpha hydrolases-like superfamily protein	MEALPEDEEY	100
AT4G13780.1	methionine-tRNA ligase, putative methionyl-tRNA synthetase, MetRS	MEDDGKSSPK	100
AT4G03560.1	two-pore channel 1	MEDPLIGRDS	100
AT2G19080.1	metaxin-like protein	MEGDQETNVY	100
AT4G24510.1	HXXXD-type acyl-transferase family protein	MEGSPVTSVR	100
AT4G15630.1	Uncharacterized protein family (UPF0497)	MEHESKNKVD	100
AT4G10060.1	Beta-glucosidase, GBA2 type family protein	MEKNGHTESE	100
AT3G45780.1	phototropin 1	MEPTEKPSTK	100
AT5G05170.1	Cellulose synthase family protein	MESEGETAGK	100
AT4G20780.1	calmodulin like 42	MESNNNEKKK	100
AT5G27670.1	histone H2A 7	MESSQATTKP	100
AT5G04430.1	binding to TOMV RNA 1L (long form)	MESTESYAAG	100
AT2G42810.1	protein phosphatase 5.2	METKNENSDV	100
AT3G04600.1	Nucleotidylyl transferase superfamily protein	MEVDKKDERE	100
AT3G16250.1	NDH-dependent cyclic electron flow 1	MGSVQLSGSG	100
AT3G05870.1	anaphase-promoting complex/cyclosome 11	MKVKILRILL	100
AT3G51490.1	tonoplast monosaccharide transporter3	MRSVVLVALA	100
AT5G44316.1	ABC transporter ABCI.9	MASLFAIGFS	99.9
AT4G36250.1	aldehyde dehydrogenase 3F1	MEAMKETVEE	99.9
AT3G27890.1	NADPH:quinone oxidoreductase	MEAVTAIKPL	99.9

AT1G70810.1	Calcium-dependent lipid-binding (CaLB domain) family protein	MEELVGLLRI	99.9
AT4G09320.1	nucleoside diphosphate kinase	MEQTFIMIKP	99.9
AT5G59870.1	histone H2A 6	MESTGKVKKA	99.9
AT3G27080.1	translocase of outer membrane 20 kDa subunit 3	MDTETEFDRI	99.8
AT4G34490.1	Adenylyl cyclase-associated protein	MEEDLIKRLE	99.8
AT4G23710.1	vacuolar ATP synthase subunit G2	MESAGIQQLL	99.8
AT5G03660.1	transcriptional activator (DUF662)	MQPTETSQPA	99.8
AT5G03430.1	phosphoadenosine phosphosulfate (PAPS) reductase family protein	MEIDKAIGES	99.7
AT5G27640.1	translation initiation factor 3B1	MEVVDIDARA	99.7
AT4G23400.1	plasma membrane intrinsic protein 1;5	MEGKEEDVNV	99.6
AT5G54310.1	ARF-GAP domain	MNEKANVSKE	99.6
AT2G43940.1	S-adenosyl-L-methionine-dependent methyltransferases superfamily protein	MENAGKATSL	99.5
AT1G13930.1	oleosin-B3-like protein	MNFISDQVKK	99.5
AT5G54430.1	Adenine nucleotide alpha hydrolases-like superfamily protein	MNPADSDHPQ	99.5
AT4G33090.1	aminopeptidase M1	MDQFKGEPRL	99.4
AT3G48990.1	AMP-dependent synthetase and ligase family protein	MDSDTLSGLL	99.4
AT4G23730.1	Galactose mutarotase-like superfamily protein	MEPSSGTGPE	99.4
AT4G11150.1	vacuolar ATP synthase subunit E1	MNDGDVSRQI	99.4
AT3G42790.1	alfin-like 3	MEGGAALYNP	99.3
AT2G34160.1	Alba DNA/RNA-binding protein	MEEITDGVNN	99.2
AT1G02090.1	COP9 signalosome complex subunit 7	MDIEQKQAEI	99
AT1G62380.1	ACC oxidase 2	MEKNMKFPVV	98.7
AT4G24800.1	MA3 domain-containing protein1	MEGFLTDQQR	98.5
AT1G04350.1	2-oxoglutarate (2OG) and Fe(II)-dependent oxygenase superfamily protein	METKEFDSYS	98.5
AT5G19140.1	aluminum induced protein with YGL and LRDR motifs	MLGIFSGAIV	98.5
AT3G53890.1	Ribosomal protein S21e	MENDAGQVTE	98.2
AT5G43830.1	aluminum induced protein with YGL and LRDR motifs	MLAVFEKTVA	96.7
AT1G29250.1	Alba DNA/RNA-binding protein	MEEITEGVNN	96.3
AT5G16100.1	Uncharacterized protein	MAGDDPKSSA	95.9
AT4G05530.1	indole-3-butyric acid response 1	MEKKLPRRLE	82.2
AT1G05010.1	ethylene-forming enzyme	MESFPIINLE	78.9
AT5G25540.1	TC-interacting domain 6	MKSGSSTLNP	75.1
AT1G20696.1	high mobility group B3	MKGAKSKAET	15.9
AT1G20693.1	high mobility group B2	MKGAKSKTET	12
AT2G17560.1	high mobility group B4	MKGGESKAEA	6.6
AT3G59970.1	methylenetetrahydrofolate reductase MTHFR1	MKVVDKIKSV	2.9
AT4G21580.1	oxidoreductase, zinc-binding dehydrogenase family protein	MKAIVISEPG	2.6
AT5G27470.1	seryl-tRNA synthetase / serine-tRNA	MLDINLFREE	2.3

	ligase		
AT3G07230.1	wound-responsive protein-like protein	MIYDVNSGLF	1.1
AT5G52650.1	RNA binding Plectin/S10 domain-containing protein	MIISEANRKE	0.6
AT3G55360.1	3-oxo-5-alpha-steroid 4-dehydrogenase family protein	MKVTVVSRSG	0.6

Table 2: List of proteins found to be less acetylated in NatB depleted plants. Detected iMet retaining N-termini with lowered NTA in NatB mutants (*naa20-1*, *naa25-1*) compared to wild-type.

	Entry	Description	N-terminus	% NTA WT	% NTA *naa20-1*	% NTA *naa25-1*
1	AT2G13360.1	Alanine:glyoxylate aminotransferase	MDYMYGPG	100	29.9	29.4
2	AT2G42810.1	Protein phosphatase 5.2	METKNENS	100	59.5	61.6
3	AT3G04600.1	Nucleotidylyl transferase superfamily protein	MEVDKKDE	100	24	14.8
4	AT3G12800.1	Short-chain dehydrogenase-reductase B	MDSPFKPD	100	35.6	22.8
5	AT3G45780.1	Phototropin 1	MEPTEKPS	100	77.5	75.6
6	AT4G13780.1	Methionyl-tRNA synthetase	MEDDGKSS	100	n/a	8.3
7	AT4G20780.1	Calmodulin like 42	MESNNNEK	100	90.1	83.8
8	AT4G24510.1	HXXXD-type acyl-transferase family protein	MEGSPVTS	100	32.5	n/a
9	AT5G04430.1	Binds to ToMV genomic RNA and prevents viral multiplication.	MESTESYA	100	n/a	64.7
10	AT5G05170.1	Cellulose synthase isomer	MESEGETA	100	47.7	n/a
11	AT5G27670.1	Translation initiation factor 3B1	MESSQATT	100	26.5	23.2
12	AT3G27890.1	NADPH:quinone oxidoreductase	MEAVTAIK	99.9	57.8	62.5
13	AT4G09320.1	Nucleoside diphosphate kinase type 1	MEQTFIMI	99.9	3.9	4.1
14	AT4G36250.1	Putative aldehyde dehydrogenase	MEAMKETV	99.9	n/a	70.6
15	AT4G23710.1	Vacuolar ATP synthase subunit G2	MESAGIQQ	99.8	39.8	39.4
16	AT4G34490.1	Cyclase asso-ciated protein 1	MEEDLIKR	99.8	6.3	3.9
17	AT5G59870.1	Histone H2A 6	MESTGKVK	99.8	n/a	15.6
18	AT5G03430.1	Phosphoadenosine phosphosulfate (PAPS) reductase family protein	MEIDKAIG	99.7	2.1	3.2

19	AT5G27640.1	Eukaryotic translation initiation factor 3 subunit B	MEVVDIDA	99.7	4.2	2.5
20	AT4G23400.1	Plasma membrane intrinsic protein 1;5	MEGKEEDV	99.6	25.1	22.2
21	AT5G54310.1	ADP-ribosylation factor GTPase-activating protein AGD5	MNEKANVS	99.6	1.8	n/a
22	AT5G54430.1	Contains a universal stress protein domain	MNPADSDH	99.5	42.5	41
23	AT3G48990.1	AMP-dependent synthetase and ligase family protein	MDSDTLSG	99.4	13.9	7.9
24	AT4G11150.1	Vacuolar H+-ATPase subunit E isoform 1	MNDGDVSR	99.4	2.2	n/a
25	AT4G23730.1	Glucose-6-phosphate 1-epimerase	MEPSSGTG	99.4	62.4	61.8
26	AT4G33090.1	Aminopeptidase M1	MDQFKGEP	99.4	15.4	20.5
27	AT3G42790.1	Alfin1-like family of nuclear-localized PHD (plant homeodomain) domain containing proteins.	MEGGAALY	99.3	37	n/a
28	AT2G34160.1	Uncharacterized protein	MEEITDGV	99.2	83.3	78.3
29	AT5G10780.1	ER membrane protein complex subunit-like protein	MDKGKAVM	99.1	88.2	85.6
30	AT1G62380.1	1-aminocyclo-propane-1-carbox-ylic oxidase (ACC oxidase)	MEKNMKFP	98.7	23.6	n/a
31	AT3G53890.1	40S ribosomal protein S21-1	MENDAGQV	98.2	5.2	12.4
32	AT1G29250.1	Alba DNA/RNA-binding protein	MEEITEGV	96.3	43.6	n/a
33	AT4G05530.1	Indole-3-butyric acid response 1	MEKKLPRR	82.2	1.9	1.6
34	AT1G20696.1	High mobility group B3 (HMGB3)	MKGAKSKA	15.9	12.3	13.1
35	AT1G20693.1	High mobility group B2 (HMGB2)	MKGAKSKT	12	7.9	8.9

705

Table 3: GO term enrichment analysis for differentially regulated genes in NatB-depleted plants. Total RNA was extracted from 17-day-old *naa20-1* and wild-type seedlings grown under short day conditions (N=4). The transcripts were analyzed via an Affimetrix® GeneChip. Differentially regulated transcripts (>1.5-fold up- or downregulated compared to wild-type, $p<0.05$) were subjected to a gene ontology enrichment analysis performed with the DAVID Bioinformatics Resources tool v.6.8 (http://david.abcc.ncifcrf.gov). Among the 494 differentially regulated transcripts, genes involved in the depicted molecular functions were significantly (>3-fold, $p<0.05$) enriched. Counts represent the number of regulated transcripts. For clarity, redundant GO terms are omitted in this table; all GO terms are available in the Supplementary Table 5.

Gene Ontology Term	Annotation	Count	Trend	Fold enriched	*P* value
defense response to bacterium	GO:0009816	6	Down	17.1	0.00
chitin metabolic/catabolic process	GO:0006030	4	Down	11.9	0.00
toxin metabolic/catabolic process	GO:0009404	5	Down	8.1	0.00
regulation of defense response	GO:0031347	6	Down	7.3	0.00
indole derivative metabolic process	GO:0042434	4	Down	7.1	0.02
polysaccharide catabolic process	GO:0000272	6	Down	6.0	0.00
response to bacterium	GO:0009617	19	Down	5.8	0.00
response to light intensity	GO:0009642	5	Down	5.1	0.02
immune response	GO:0006955	20	Down	5.1	0.00
cell death	GO:0008219	17	Down	5.0	0.00
response to chitin	GO:0010200	8	Down	4.7	0.00
response to oxidative stress	GO:0006979	15	Down	3.9	0.00
response to salicylic acid stimulus	GO:0009751	7	Down	3.5	0.02
defense response	GO:0006952	45	Down	3.2	0.00
zinc ion transport	GO:0006829	4	Up	27.9	0.00
transition metal ion transport	GO:0000041	5	Up	10.0	0.00
lipid localization	GO:0010876	7	Up	6.2	0.00
lipid transport	GO:0006869	5	Up	5.0	0.02

Figures

Figure 1

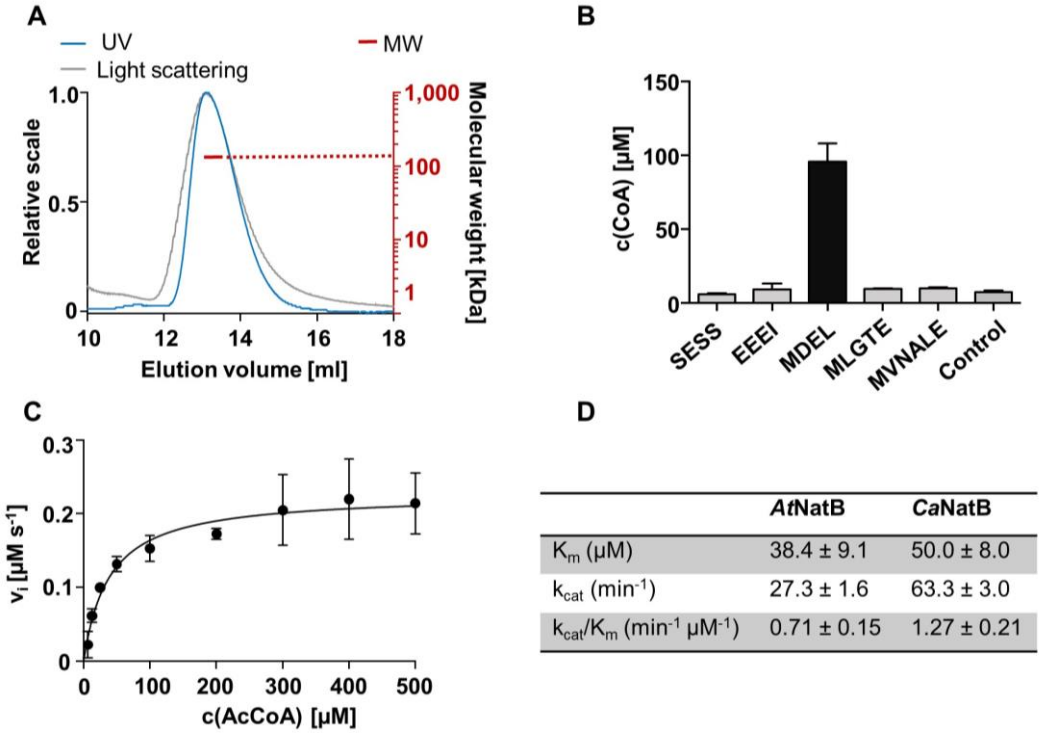

	*At*NatB	*Ca*NatB
K_m (µM)	38.4 ± 9.1	50.0 ± 8.0
k_{cat} (min^{-1})	27.3 ± 1.6	63.3 ± 3.0
k_{cat}/K_m (min^{-1} $µM^{-1}$)	0.71 ± 0.15	1.27 ± 0.21

Figure 1. *At*NatB acetylates MDEL peptides *in vitro*. A Size-exclusion chromatography coupled to multi-angle light scattering (SEC-MALS) analyses of *At*NatB. The UV-signal (blue) of the corresponding SEC chromatogram is shown together with the light scattering signal (grey) and the mass distribution (red bar). The experimentally determined molecular weight (MW) is 132.1 kDa and fits well to the theoretical calculated molecular weight of 132.5 kDa for both subunits. **B** Substrate specificity of *At*NatB tested with five different peptides. The peptides SESS, EEEI, MDEL, MLGTE and MVNALE were previously identified as NatA, Naa10/Naa80, NatB and NatC/E/F substrates. The control reaction was performed in the absence of peptides. **C** Michaelis-Menten plot of the acetylation of MDEL catalyzed by *At*NatB. **B-C** The reactions were performed in triplicate and error bars represent the standard deviation. **D** Enzymatic parameters of *At*NatB compared to its *Candida albicans* homolog (*Ca*NatB, Hong et al. (2017)).

737 **Figure 2**

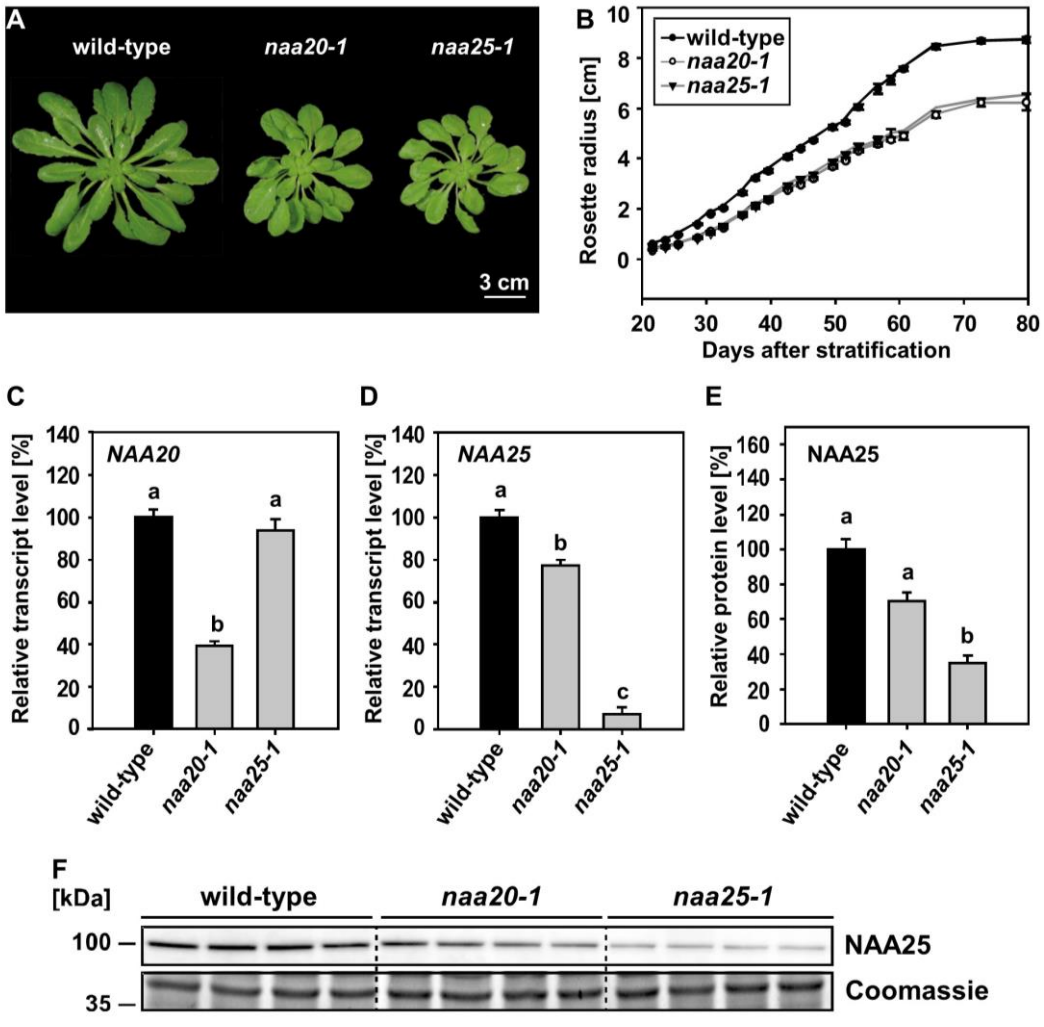

738

739 **Figure 2. Depletion of NAA20 and NAA25 results in growth retardation. A**
740 Representative growth phenotypes of wild-type, *naa20-1* and *naa25-1* plants grown
741 for six weeks under short day conditions. **B** Growth curve based on the rosette radius
742 20-79 days after stratification. **C,D** Quantification of relative *NAA20* (**C**) and *NAA25*
743 (**D**) transcript levels via qRT-PCR in the leaves of six-week-old plants. **E**
744 Quantification of the NAA25 protein amount detected via a specific antiserum in
745 soluble leaf protein extracts of six-week-old plants grown under short-day conditions
746 (**F**) as specified in material and methods. **F** Immunological detection of *At*NAA25 for
747 quantification shown in **E** (n=4). The blot shows four biological replicates for each
748 genotype grown under identical conditions. Data given as means ± s.e. Different
749 letters indicate individual groups identified by pairwise multiple comparisons with a
750 Holm-Sidak, One-way ANOVA ($p<0.05$, $n\geq3$).

751

752

Figure 3

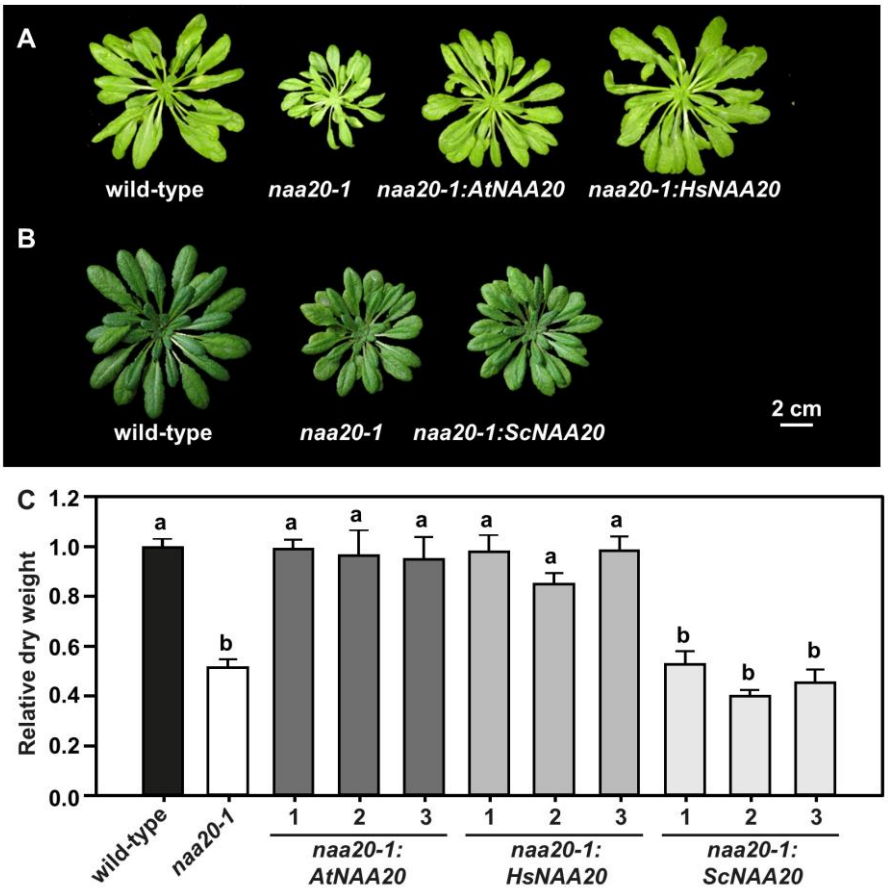

Figure 3. The Arabidopsis *naa20-1* mutant can be complemented with the *Hs*NAA20 orthologue. Representative growth phenotypes of plants grown for eight weeks under short day conditions. Plants depleted in NAA20 were transformed either with **A** the endogenous Arabidopsis *NAA20* (*naa20-1:AtNAA20*) or the respective homologues from humans (*naa20-1*:*Hs*NAA20) or **B** yeast (*naa20-1*:*ScNAA20*). Scale bar, 2 cm. **C** Relative rosette dry weight of the indicated plants after eight weeks of growth. For each transformation, three representative independent lines are shown. Data given as means ± s.e. Different letters indicate individual groups identified by pairwise multiple comparisons with a Holm-Sidak, One-way ANOVA ($p<0.05$, $n\geq3$).

Figure 4

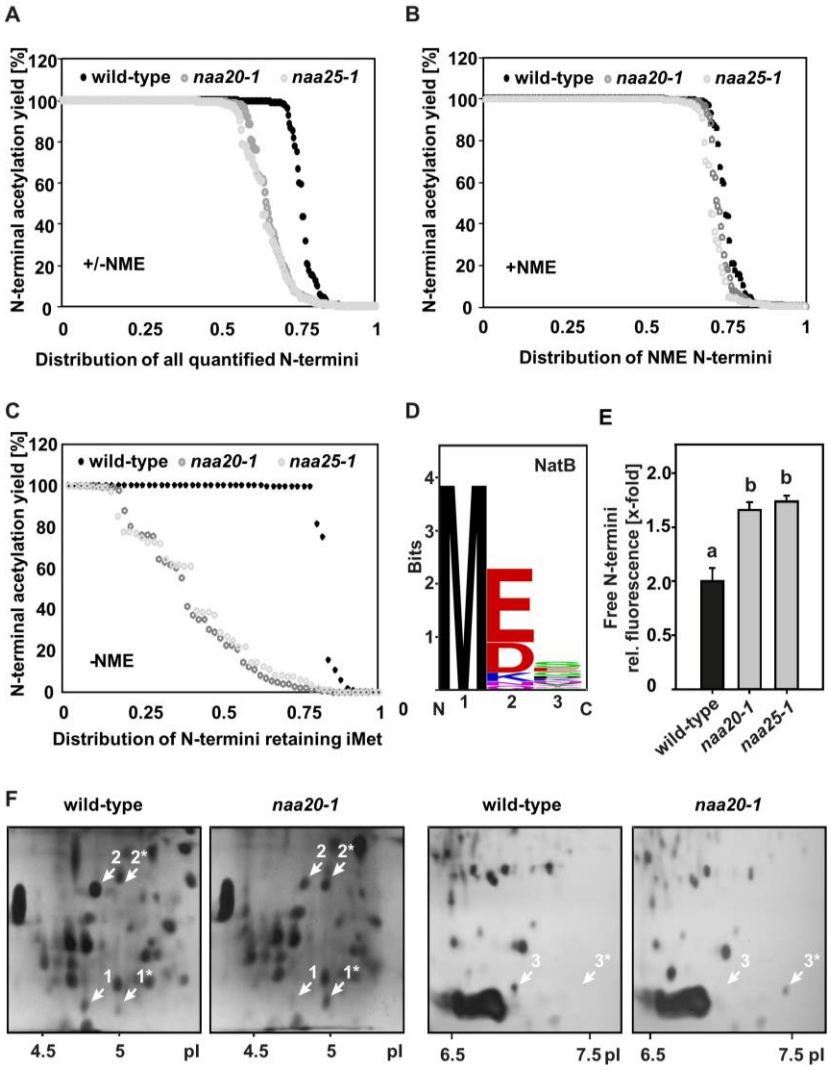

Figure 4. The Arabidopsis NatB complex acetylates N-termini which retain their iMet. A-C The acetylation level of protein N-termini was studied in leaves of six-week-old plants grown under short-day conditions on soil. The mass spectrometry analysis depicts the acetylation levels of all detected N-termini (**A**) as well as N-termini with (**B**) or without (**C**) N-terminal methionine excision (NME). **D** Based on the identified substrates, the NatB target consensus sequence was determined using weblogo.berkeley.edu. The size of the letter code corresponds to the relative amino acid frequency at positions one to ten. **E** Quantification of the relative global amount of free N-termini in soluble protein extracts isolated from leaves of six-week-old plants. Data given as means ± s.e. Different letters indicate individual groups identified by pairwise multiple comparisons with a Holm-Sidak, One-way ANOVA ($p<0.05$, $n\geq3$). **F** Section of 2D-PAGE gels comparing soluble protein extracts of nine-week-old wild-type and *naa20-1* plants. Arrows mark proteins with a basic shift in the *naa20-1* mutant, indicating a loss of NTA. Proteins were identified by mass spectrometry. 1/1* salt stress-related protein (AT1G13930, MD), 2/2* nucleoside diphosphate kinase 1 (AT4G09320, ME), 3/3* membrane-associated progesterone binding protein (AT2G24940, ME).

Figure 5

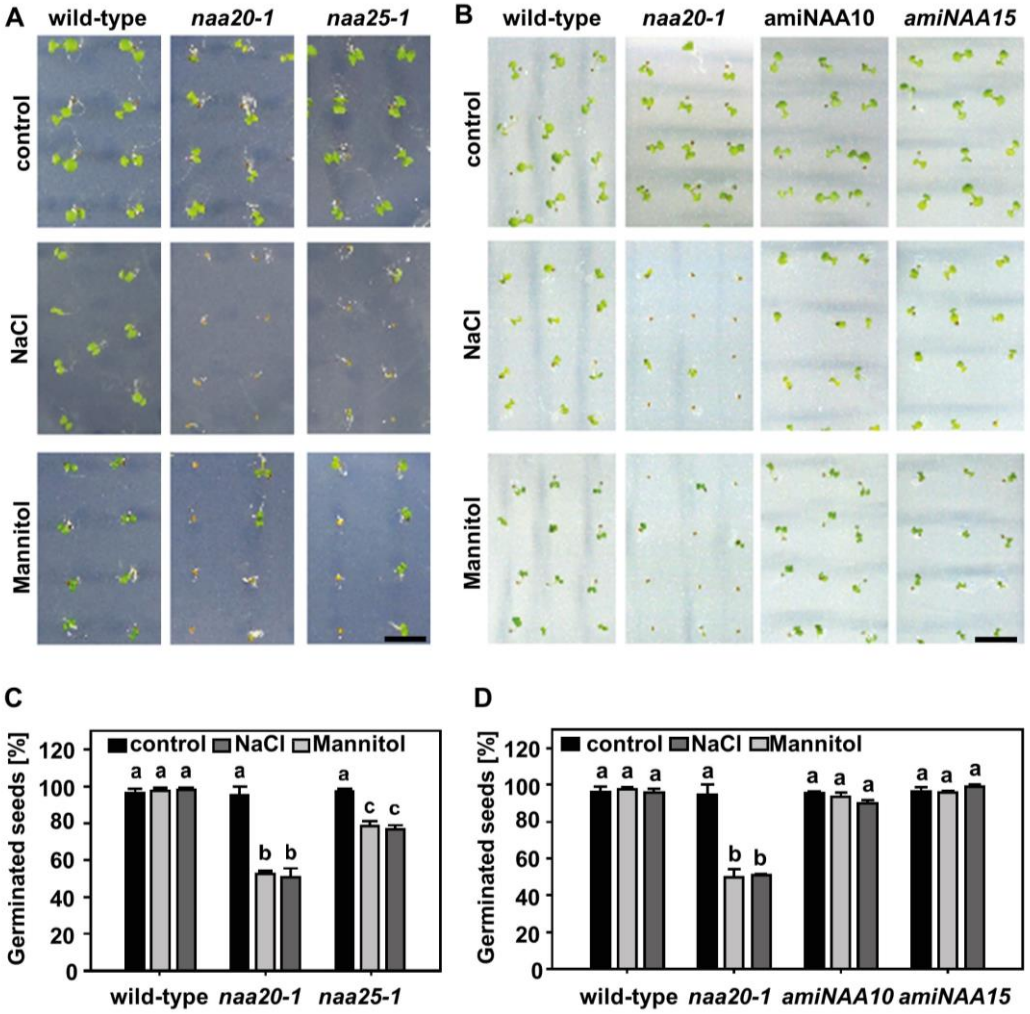

Figure 5. NatB mutants are sensitive to salt and osmotic stress. Seeds of mutants depleted in subunits of NatB or NatA were surface sterilized, stratified for two days and germinated on 1xMS medium (Control) or medium supplemented with 100 mM NaCl (NaCl) or 3 % mannitol (Mannitol), respectively. Germination of plants was evaluated after seven days of growth under short day conditions. **A, B** Representative sections of germinated and non-germinated seeds. Scale bar, 5 mm. **C,D** Quantification of corresponding germination rates. Data given as means ± s.e. Different letters indicate individual groups identified by pairwise multiple comparisons with a Holm-Sidak, One-way ANOVA ($p<0.05$, $n=3$, $1n\geq30$ seeds).

Supplement

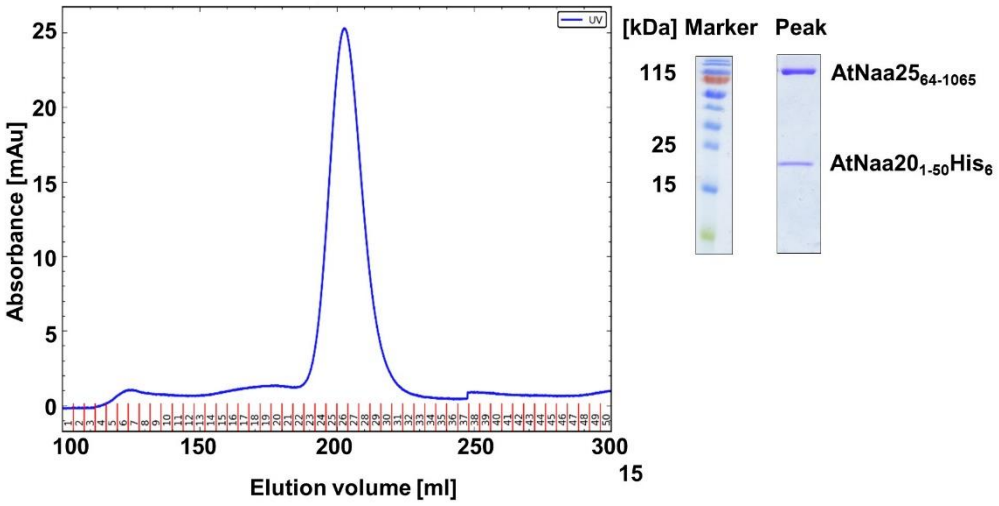

Supplementary figure 1. Size-exclusion chromatography profile of purified *At*NatB.

Size-exclusion chromatography of co-purified *At*NAA25$_{64-1065}$ and *AtNAA20*$_{1-150}$His$_6$ revealed a single peak. The corresponding protein fraction contains both NatB subunits as shown by SDS-PAGE followed by Coomassie staining.

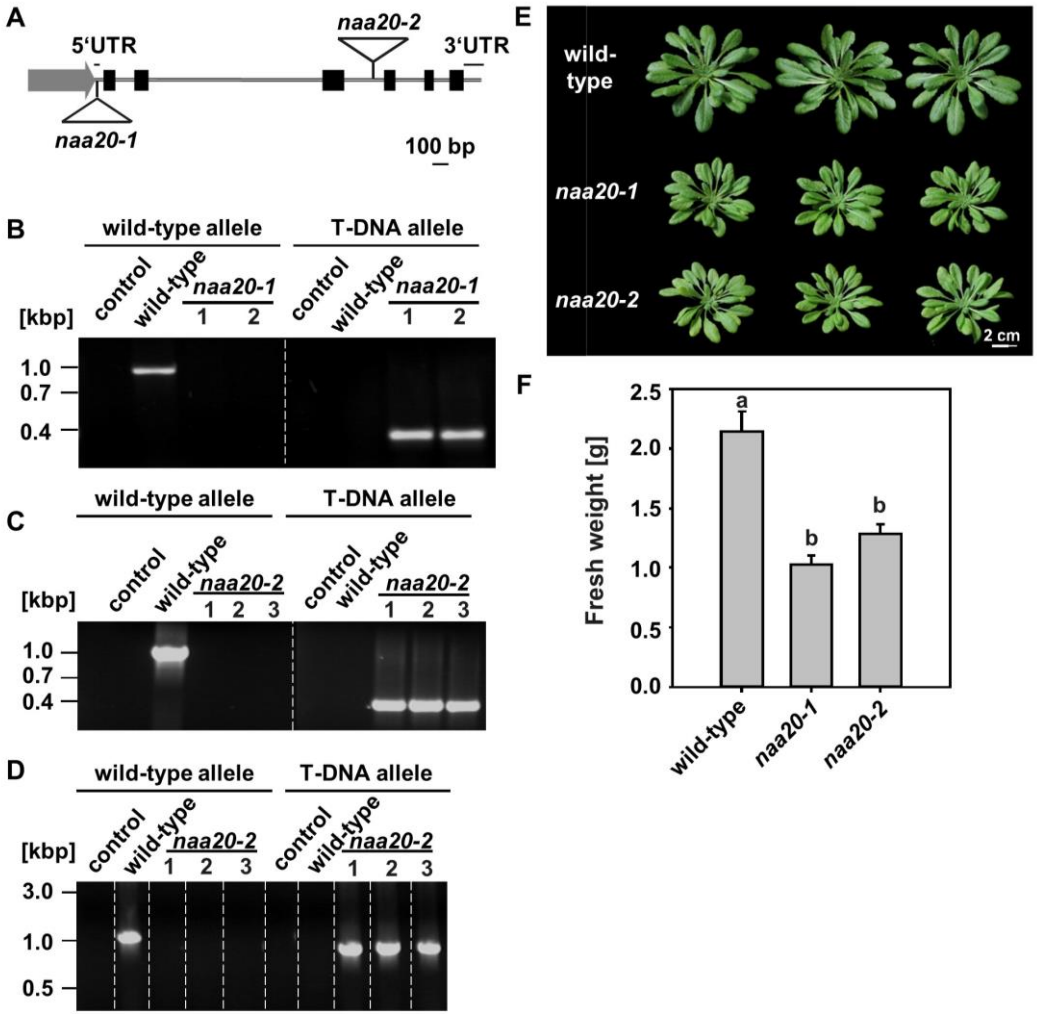

Supplementary figure 2. Characterization of different *naa20* T-DNA insertion mutants. A Schematic depiction of the *NAA20* gene structure. Black rectangles represent exons and lines depict intronic regions. Triangles indicate the site of insertion in the corresponding T-DNA lines. **B,C,D** Genotyping of homozygous *naa20-1*, *naa20-2* and *naa25-1* plants using the primer combinations given in supplementary table 1. Dashed lines indicate borders between sections from different parts of the gel. **E** Representative rosettes of eight-week-old wild-type, *naa20-1* and *naa20-2* plants grown under short day conditions. **F** Quantification of rosette fresh weights of eight-week-old soil grown plants. Different letters indicate individual groups identified by pairwise multiple comparisons with a Holm-Sidak, One-way ANOVA ($p<0.01$, $n=6$).

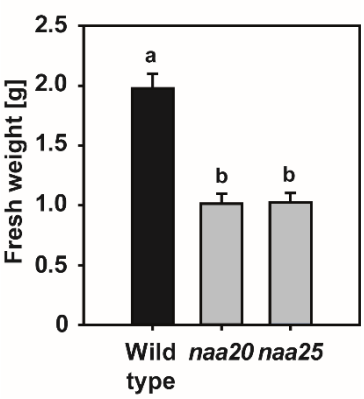

Supplementary figure 3. Rosette fresh weight of NatB depleted plants. Analyzed were seven-week-old plants grown under short-day conditions. Data represent mean ±s.e. Different letters indicate individual groups identified by pairwise multiple comparisons with a Holm-Sidak, One-way ANOVA ($p<0.05$, $n\geq8$).

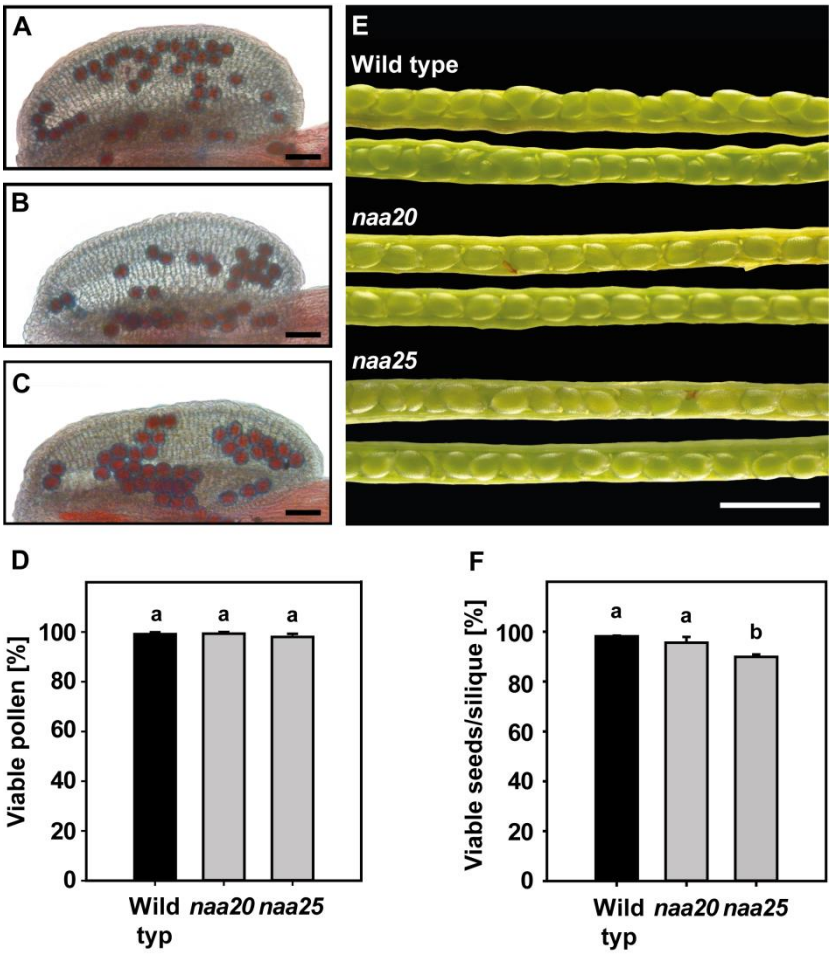

826

827 **Supplementary figure 4. Embryo development in NatB depleted plants.** Pollen
828 viability staining (Alexander, 1969) in anthers of wild-type (**A**), *naa20-1* (**B**) and
829 *naa25-1* (**C**) plants. Viable pollen shows a purple staining of the protoplasm and a
830 green stained pollen wall. Aborted pollen appears green due to released protoplasm
831 (n=4, 40 pollen grains each). Scale bar: 50 µm. **D** Dissected siliques. Scale bar:
832 1 mm. **F** Relative number of viable seeds per silique. Data given as means ±s.e.
833 Different letters indicate individual groups identified by pairwise multiple comparisons
834 with a Holm-Sidak, One-way ANOVA ($p<0.05$, $n\geq3$, 6 siliques each).

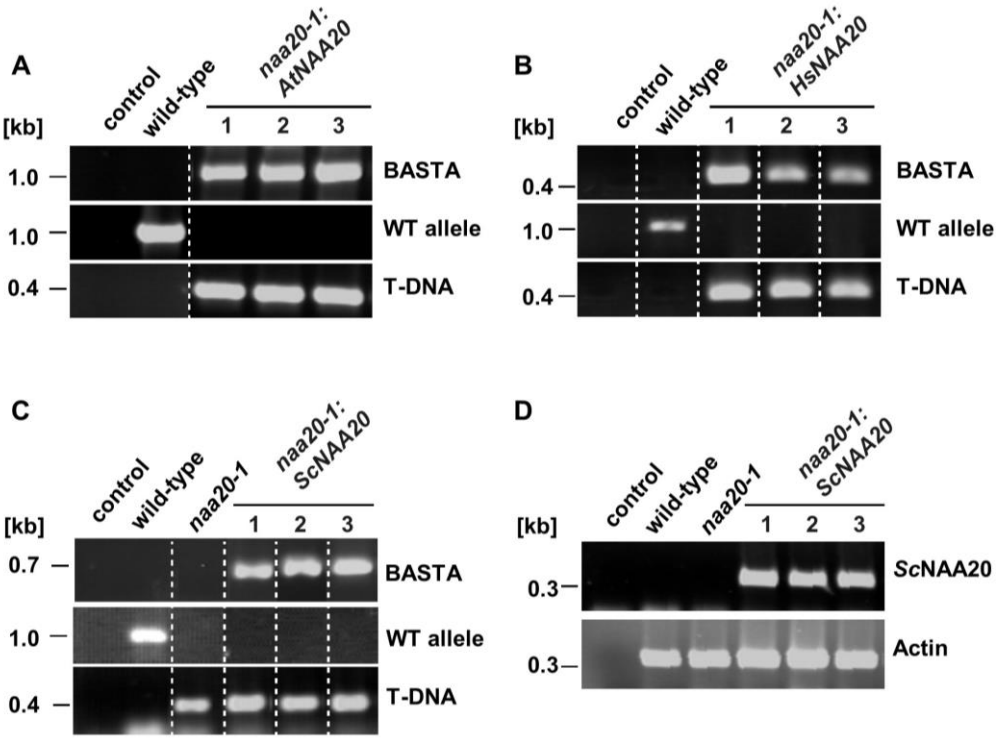

Supplementary figure 5. Confirmation of *naa20-1* transformation and *ScNAA20* expression. A-C Genotyping of *naa20-1* transformants to verify the integration of the corresponding *AtNAA20* (**A**), *HsNAA20* (**B**) or *ScNAA20* (**C**) expressing constructs. "BASTA" indicates the amplification of the glufosinate resistance marker gene. Genomic DNA from wild-type and a non-template control were used as negative controls. **D** Semi-quantitative RT-PCR of *ScNAA20* transcription in corresponding *naa20-1* transformants. Transcription of actin was used as internal control.

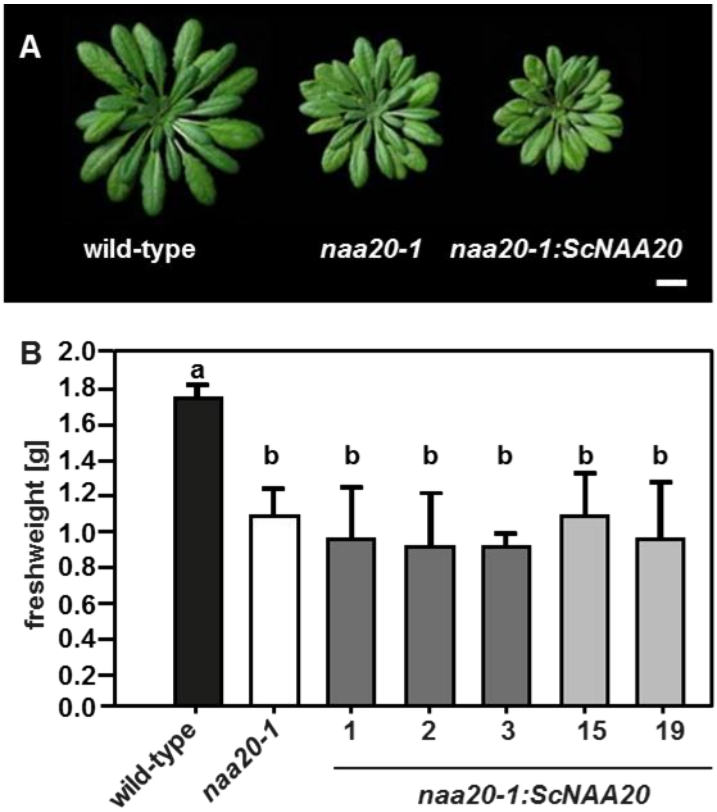

Supplementary figure 6. The Arabidopsis *naa20-1* mutant cannot be complemented with the *Sc*NAA20 orthologue. **A** Representative growth phenotypes of plants grown for eight weeks under short day conditions. Plants depleted in NAA20 were transformed with *ScNAA20* (*naa20-1*::*ScNAA20*). Five independent lines are shown. Scale bar, 2 cm. **B** Rosette fresh weight of the indicated plants after eight weeks of growth. Data given as means ± s.e. Different letters indicate individual groups identified by pairwise multiple comparisons with a Holm-Sidak, One-way ANOVA ($p<0.05$, $n\geq10$-12).

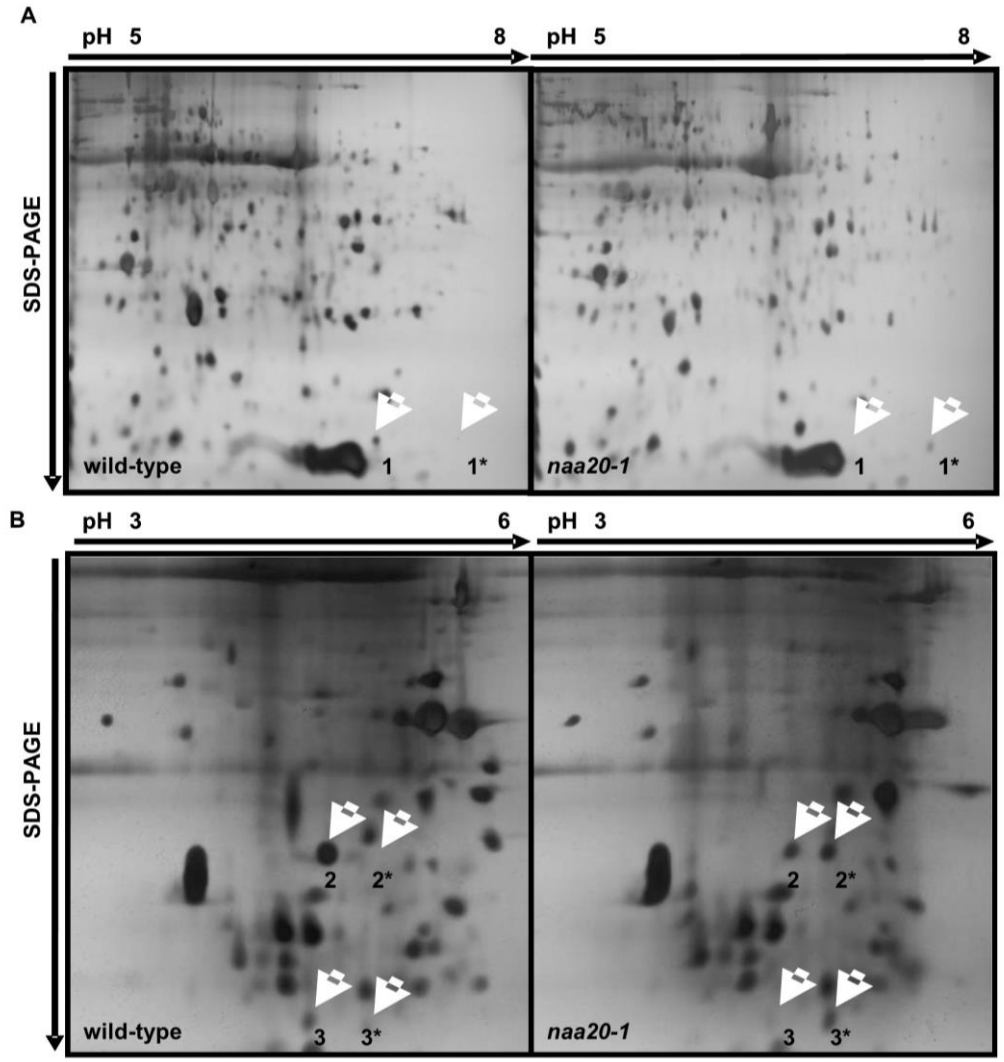

Supplementary figure 7. 2D-PAGE gels comparing soluble protein extracts of nine-week-old wild-type and *naa20-1* plants. Selected areas of these gels have been shown in Figure 4F. Arrows mark proteins with a basic shift in the *naa20-1* mutant, indicating a loss of NTA. Proteins were identified by mass spectrometry. 1/1* salt stress-related protein (AT1G13930, MD), 2/2* nucleoside diphosphate kinase 1 (AT4G09320, ME), 3/3* membrane-associated progesterone binding protein (AT2G24940, ME).

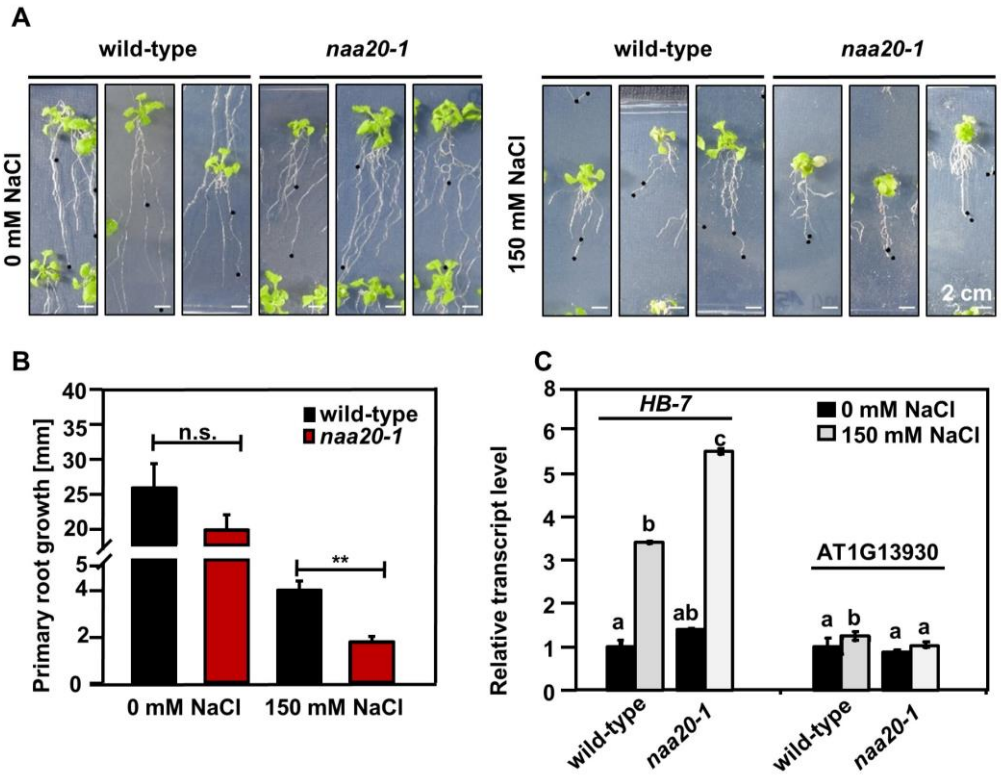

Supplementary figure 8. Four-weeks-old NatB mutants are sensitive to salt stress. Seeds of wild-type and *naa20-1* mutants were surface sterilized, stratified for two days and grown on ½ x MS medium supplemented with 1 % sucrose for two-weeks under short-day conditions. Plants were transferred to the same medium (control) or medium supplemented with 150 mM NaCl and the growth of the primary root was evaluated after two-weeks. **A** Habitus of representative wild-type and *naa20-1* plants. The upper dot indicates the location of the root tip directly after the transfer of plants. The lower dot labels the position of the root after 2 weeks of high salt treatment. Scale bar, 2 cm. **B** Quantification of root growth during the high salt treatment. Data given as means ± s.e. Asterisks indicate statistically significant differences between *naa20-1* when compared to wild-type determined with the students t-test ($p<0.05$, $n\geq14$ individual plants). **C** Transcript levels of the high salt-stress marker, *HB-7* (AT2G46680), and AT1G13930 in wild-type and *naa20-1* plants shown in **A** as determined by qRT-PCR. Primers for specific amplification are listed in the Supplementary Table 6. PP2A (AT1G69960) and MON1 (AT2G28390) have been used as reference. Different letters indicate individual groups identified by pairwise multiple comparisons with a Holm-Sidak One-way ANOVA ($p<0.05$, $n=4$ pools of six plants each).

References

Aksnes H, Drazic A, Marie M, Arnesen T (2016) First Things First: Vital Protein Marks by N-Terminal Acetyltransferases. Trends Biochem Sci **41:** 746-760

Aksnes H, Hole K, Arnesen T (2015a) Molecular, cellular, and physiological significance of N-terminal acetylation. Int Rev Cell Mol Biol **316:** 267-305

Aksnes H, Ree R, Arnesen T (2019) Co-translational, Post-translational, and Non-catalytic Roles of N-Terminal Acetyltransferases. Mol Cell **73:** 1097-1114

Aksnes H, Van Damme P, Goris M, Starheim KK, Marie M, Stove SI, Hoel C, Kalvik TV, Hole K, Glomnes N, Furnes C, Ljostveit S, Ziegler M, Niere M, Gevaert K, Arnesen T (2015b) An organellar nalpha-acetyltransferase, naa60, acetylates cytosolic N termini of transmembrane proteins and maintains Golgi integrity. Cell Rep **10:** 1362-1374

Alexander MP (1969) Differential staining of aborted and nonaborted pollen. Stain Technol **44:** 117-122

Alonso JM, Stepanova AN, Leisse TJ, Kim CJ, Chen H, Shinn P, Stevenson DK, Zimmerman J, Barajas P, Cheuk R, Gadrinab C, Heller C, Jeske A, Koesema E, Meyers CC, Parker H, Prednis L, Ansari Y, Choy N, Deen H, Geralt M, Hazari N, Hom E, Karnes M, Mulholland C, Ndubaku R, Schmidt I, Guzman P, Aguilar-Henonin L, Schmid M, Weigel D, Carter DE, Marchand T, Risseeuw E, Brogden D, Zeko A, Crosby WL, Berry CC, Ecker JR (2003) Genome-wide insertional mutagenesis of Arabidopsis thaliana. Science **301:** 653-657

Ametzazurra A, Gazquez C, Lasa M, Larrea E, Prieto J, Aldabe R (2009) Characterization of the human Nalpha-terminal acetyltransferase B enzymatic complex. BMC Proc **3 Suppl 6:** S4

Ametzazurra A, Larrea E, Civeira MP, Prieto J, Aldabe R (2008) Implication of human N-alpha-acetyltransferase 5 in cellular proliferation and carcinogenesis. Oncogene **27:** 7296-7306

Arnesen T (2011) Towards a functional understanding of protein N-terminal acetylation. PLoS Biol **9:** e1001074

Arnesen T, Gromyko D, Kagabo D, Betts MJ, Starheim KK, Varhaug JE, Anderson D, Lillehaug JR (2009a) A novel human NatA Nalpha-terminal acetyltransferase complex: hNaa16p-hNaa10p (hNat2-hArd1). BMC Biochem **10:** 15

Arnesen T, Van Damme P, Polevoda B, Helsens K, Evjenth R, Colaert N, Varhaug JE, Vandekerckhove J, Lillehaug JR, Sherman F, Gevaert K (2009b) Proteomics analyses reveal the evolutionary conservation and divergence of N-terminal acetyltransferases from yeast and humans. Proc Natl Acad Sci U S A **106:** 8157-8162

Bernal-Perez LF, Prokai L, Ryu Y (2012) Selective N-terminal fluorescent labeling of proteins using 4-chloro-7-nitrobenzofurazan: A method to distinguish protein N-terminal acetylation. Analytical Biochemistry **428:** 13-15

Bienvenut WV, Giglione C, Meinnel T (2017a) SILProNAQ: A Convenient Approach for Proteome-Wide Analysis of Protein N-Termini and N-Terminal Acetylation Quantitation. Methods Mol Biol **1574:** 17-34

Bienvenut WV, Scarpelli JP, Dumestier J, Meinnel T, Giglione C (2017b) EnCOUNTer: a parsing tool to uncover the mature N-terminus of organelle-targeted proteins in complex samples. BMC Bioinformatics **18:** 182

Bienvenut WV, Sumpton D, Martinez A, Lilla S, Espagne C, Meinnel T, Giglione C (2012) Comparative Large Scale Characterization of Plant versus Mammal Proteins Reveals Similar and Idiosyncratic N-α-Acetylation Features. Molecular & Cellular Proteomics **11:** M111.015131

Blum H, Beier H, Gross HJ (1987) Improved silver staining of plant proteins, RNA and DNA in polyacrylamide gels. Electrophoresis **8:** 93-99

Bradford MM (1976) A rapid and sensitive method for the quantitation of microgram quantities of protein utilizing the principle of protein-dye binding. Anal Biochem **72:** 248-254

Caesar R, Blomberg A (2004) The stress-induced Tfs1p requires NatB-mediated acetylation to inhibit carboxypeptidase Y and to regulate the protein kinase A pathway. J Biol Chem **279:** 38532-38543

Caesar R, Warringer J, Blomberg A (2006) Physiological importance and identification of novel targets for the N-terminal acetyltransferase NatB. Eukaryot Cell **5:** 368-378

Casey JP, Støve SI, McGorrian C, Galvin J, Blenski M, Dunne A, Ennis S, Brett F, King MD, Arnesen T, Lynch SA (2015) NAA10 mutation causing a novel intellectual disability syndrome with Long QT due to N-terminal acetyltransferase impairment. Scientific Reports **5:** 16022

Chen Z, Zhao P-X, Miao Z-Q, Qi G-F, Wang Z, Yuan Y, Ahmad N, Cao M-J, Hell R, Wirtz M, Xiang C-B (2019) SULTR3s Function in Chloroplast Sulfate Uptake and Affect ABA Biosynthesis and the Stress Response. Plant Physiol **180:** 593-604

Czechowski T, Stitt M, Altmann T, Udvardi MK, Scheible WR (2005) Genome-wide identification and testing of superior reference genes for transcript normalization in Arabidopsis. Plant Physiol **139:** 5-17

Dinh TV, Bienvenut WV, Linster E, Feldman-Salit A, Jung VA, Meinnel T, Hell R, Giglione C, Wirtz M (2015) Molecular identification and functional characterization of the first N^{a}-acetyltransferase in plastids by global acetylome profiling. Proteomics **15:** 2426-2435

Drazic A, Aksnes H, Marie M, Boczkowska M, Varland S, Timmerman E, Foyn H, Glomnes N, Rebowski G, Impens F, Gevaert K, Dominguez R, Arnesen T (2018) NAA80 is actin's N-terminal acetyltransferase and regulates cytoskeleton assembly and cell motility. Proc Natl Acad Sci U S A

Dupree P, Sherrier DJ (1998) The plant Golgi apparatus. Biochim Biophys Acta **1404:** 259-270

Falb M, Aivaliotis M, Garcia-Rizo C, Bisle B, Tebbe A, Klein C, Konstantinidis K, Siedler F, Pfeiffer F, Oesterhelt D (2006) Archaeal N-terminal protein maturation commonly involves N-terminal acetylation: a large-scale proteomics survey. J Mol Biol **362:** 915-924

Ferrandez-Ayela A, Micol-Ponce R, Sanchez-García AB, Alonso-Peral MM, Micol JL, Ponce MR (2013) Mutation of an Arabidopsis NatB N-Alpha-Terminal Acetylation Complex Component Causes Pleiotropic Developmental Defects. PLoS ONE **8:** e80697, 80691-80611

Frottin F, Martinez A, Peynot P, Mitra S, Holz RC, Giglione C, Meinnel T (2006) The proteomics of N-terminal methionine cleavage. Mol Cell Proteomics **5:** 2336-2349

Giglione C, Fieulaine S, Meinnel T (2015) N-terminal protein modifications: Bringing back into play the ribosome. Biochimie

Heeg C, Kruse C, Jost R, Gutensohn M, Ruppert T, Wirtz M, Hell R (2008) Analysis of the Arabidopsis *O*-acetylserine(thiol)lyase gene family demonstrates compartment-specific differences in the regulation of cysteine synthesis. Plant Cell **20:** 168-185

Helbig AO, Rosati S, Pijnappel PW, van Breukelen B, Timmers MH, Mohammed S, Slijper M, Heck AJ (2010) Perturbation of the yeast N-acetyltransferase NatB induces elevation of protein phosphorylation levels. BMC Genomics **11:** 685

Hong H, Cai Y, Zhang S, Ding H, Wang H, Han A (2017) Molecular Basis of Substrate Specific Acetylation by N-Terminal Acetyltransferase NatB. Structure **25:** 641-649 e643

Huang da W, Sherman BT, Lempicki RA (2009a) Bioinformatics enrichment tools: paths toward the comprehensive functional analysis of large gene lists. Nucleic Acids Res **37:** 1-13

Huang da W, Sherman BT, Lempicki RA (2009b) Systematic and integrative analysis of large gene lists using DAVID bioinformatics resources. Nat Protoc **4:** 44-57

Kaundal R, Saini R, Zhao PX (2010) Combining Machine Learning and Homology-Based Approaches to Accurately Predict Subcellular Localization in Arabidopsis. Plant Physiology **154:** 36-54

Linster E, Stephan I, Bienvenut WV, Maple-Grodem J, Myklebust LM, Huber M, Reichelt M, Sticht C, Geir Moller S, Meinnel T, Arnesen T, Giglione C, Hell R, Wirtz M (2015) Downregulation of N-terminal acetylation triggers ABA-mediated drought responses in Arabidopsis. Nat Commun **6:** 7640

Linster E, Wirtz M (2018) N-terminal acetylation: an essential protein modification emerges as an important regulator of stress responses. J Exp Bot **69:** 4555-4568

Nguyen KT, Kim JM, Park SE, Hwang CS (2019) N-terminal methionine excision of proteins creates tertiary destabilizing N-degrons of the Arg/N-end rule pathway. J Biol Chem **294:** 4464-4476

Nilsson OB, Hedman R, Marino J, Wickles S, Bischoff L, Johansson M, Muller-Lucks A, Trovato F, Puglisi JD, O'Brien EP, Beckmann R, von Heijne G (2015) Cotranslational Protein Folding inside the Ribosome Exit Tunnel. Cell Rep **12:** 1533-1540

Noji M, Inoue K, Kimura N, Gouda A, Saito K (1998) Isoform-dependent differences in feedback regulation and subcellular localization of serine acetyltransferase involved in cysteine biosynthesis from Arabidopsis thaliana. J Biol Chem **273:** 32739-32745

Pesaresi P, Gardner NA, Masiero S, Dietzmann A, Eichacker L, Wickner R, Salamini F, Leister D (2003) Cytoplasmic N-terminal protein acetylation is required for efficient photosynthesis in Arabidopsis. Plant Cell **15:** 1817-1832

Pierre M, Traverso JA, Boisson B, Domenichini S, Bouchez D, Giglione C, Meinnel T (2007) N-myristoylation regulates the SnRK1 pathway in Arabidopsis. Plant Cell **19:** 2804-2821

Polevoda B, Arnesen T, Sherman F (2009) A synopsis of eukaryotic Nalpha-terminal acetyltransferases: nomenclature, subunits and substrates. BMC Proc **3 Suppl 6:** S2

Polevoda B, Brown S, Cardillo TS, Rigby S, Sherman F (2008) Yeast N(alpha)-terminal acetyltransferases are associated with ribosomes. J Cell Biochem **103:** 492-508

Polevoda B, Cardillo TS, Doyle TC, Bedi GS, Sherman F (2003) Nat3p and Mdm20p are required for function of yeast NatB Nalpha-terminal acetyltransferase and of actin and tropomyosin. J Biol Chem **278:** 30686-30697

Polevoda B, Sherman F (2003) N-terminal acetyltransferases and sequence requirements for N-terminal acetylation of eukaryotic proteins. J Mol Biol **325:** 595-622

Ree R, Myklebust LM, Thiel P, Foyn H, Fladmark KE, Arnesen T (2015) The N-terminal acetyltransferase Naa10 is essential for zebrafish development. Biosci Rep **35**

Reid DW, Nicchitta CV (2015) Diversity and selectivity in mRNA translation on the endoplasmic reticulum. Nature reviews. Molecular cell biology **16:** 221-231

Rosso MG, Li Y, Strizhov N, Reiss B, Dekker K, Weisshaar B (2003) An Arabidopsis thaliana T-DNA mutagenized population (GABI-Kat) for flanking sequence tag-based reverse genetics. Plant Mol Biol **53:** 247-259

Sessions A, Burke E, Presting G, Aux G, McElver J, Patton D, Dietrich B, Ho P, Bacwaden J, Ko C, Clarke JD, Cotton D, Bullis D, Snell J, Miguel T, Hutchison D, Kimmerly B, Mitzel T, Katagiri F, Glazebrook J, Law M, Goff SA (2002) A high-throughput Arabidopsis reverse genetics system. Plant Cell **14:** 2985-2994

Singer JM, Shaw JM (2003) Mdm20 protein functions with Nat3 protein to acetylate Tpm1 protein and regulate tropomyosin-actin interactions in budding yeast. Proc Natl Acad Sci U S A **100:** 7644-7649

Starheim KK, Arnesen T, Gromyko D, Ryningen A, Varhaug JE, Lillehaug JR (2008) Identification of the human N(alpha)-acetyltransferase complex B (hNatB): a complex important for cell-cycle progression. Biochem J **415:** 325-331

Van Damme P, Lasa M, Polevoda B, Gazquez C, Elosegui-Artola A, Kim DS, De Juan-Pardo E, Demeyer K, Hole K, Larrea E, Timmerman E, Prieto J, Arnesen T, Sherman F, Gevaert K, Aldabe R (2012) N-terminal acetylome analyses and functional insights of the N-terminal acetyltransferase NatB. Proc Natl Acad Sci U S A **109:** 12449-12454

Xu F, Huang Y, Li L, Gannon P, Linster E, Huber M, Kapos P, Bienvenut W, Polevoda B, Meinnel T, Hell R, Giglione C, Zhang Y, Wirtz M, Chen S, Li X (2015) Two N-terminal acetyltransferases antagonistically regulate the stability of a nod-like receptor in Arabidopsis. Plant Cell **27:** 1547-1562

Parsed Citations

Aksnes H, Drazic A, Marie M, Arnesen T (2016) First Things First: Vital Protein Marks by N-Terminal Acetyltransferases. Trends Biochem Sci 41: 746-760

Pubmed: Author and Title
Google Scholar: Author Only Title Only Author and Title

Aksnes H, Hole K, Arnesen T (2015a) Molecular, cellular, and physiological significance of N-terminal acetylation. Int Rev Cell Mol Biol 316: 267-305

Pubmed: Author and Title
Google Scholar: Author Only Title Only Author and Title

Aksnes H, Ree R, Arnesen T (2019) Co-translational, Post-translational, and Non-catalytic Roles of N-Terminal Acetyltransferases. Mol Cell 73: 1097-1114

Pubmed: Author and Title
Google Scholar: Author Only Title Only Author and Title

Aksnes H, Van Damme P, Goris M, Starheim KK, Marie M, Stove SI, Hoel C, Kalvik TV, Hole K, Glomnes N, Furnes C, Ljostveit S, Ziegler M, Niere M, Gevaert K, Arnesen T (2015b) An organellar nalpha-acetyltransferase, naa60, acetylates cytosolic N termini of transmembrane proteins and maintains Golgi integrity. Cell Rep 10: 1362-1374

Pubmed: Author and Title
Google Scholar: Author Only Title Only Author and Title

Alexander MP (1969) Differential staining of aborted and nonaborted pollen. Stain Technol 44: 117-122

Pubmed: Author and Title
Google Scholar: Author Only Title Only Author and Title

Alonso JM, Stepanova AN, Leisse TJ, Kim CJ, Chen H, Shinn P, Stevenson DK, Zimmerman J, Barajas P, Cheuk R, Gadrinab C, Heller C, Jeske A, Koesema E, Meyers CC, Parker H, Prednis L, Ansari Y, Choy N, Deen H, Geralt M, Hazari N, Hom E, Karnes M, Mulholland C, Ndubaku R, Schmidt I, Guzman P, Aguilar-Henonin L, Schmid M, Weigel D, Carter DE, Marchand T, Risseeuw E, Brogden D, Zeko A, Crosby WL, Berry CC, Ecker JR (2003) Genome-wide insertional mutagenesis of Arabidopsis thaliana. Science 301: 653-657

Pubmed: Author and Title
Google Scholar: Author Only Title Only Author and Title

Ametzazurra A, Gazquez C, Lasa M, Larrea E, Prieto J, Aldabe R (2009) Characterization of the human Nalpha-terminal acetyltransferase B enzymatic complex. BMC Proc 3 Suppl 6: S4

Pubmed: Author and Title
Google Scholar: Author Only Title Only Author and Title

Ametzazurra A, Larrea E, Civeira MP, Prieto J, Aldabe R (2008) Implication of human N-alpha-acetyltransferase 5 in cellular proliferation and carcinogenesis. Oncogene 27: 7296-7306

Pubmed: Author and Title
Google Scholar: Author Only Title Only Author and Title

Arnesen T (2011) Towards a functional understanding of protein N-terminal acetylation. PLoS Biol 9: e1001074

Pubmed: Author and Title
Google Scholar: Author Only Title Only Author and Title

Arnesen T, Gromyko D, Kagabo D, Betts MJ, Starheim KK, Varhaug JE, Anderson D, Lillehaug JR (2009a) A novel human NatA Nalpha-terminal acetyltransferase complex: hNaa16p-hNaa10p (hNat2-hArd1). BMC Biochem 10: 15

Pubmed: Author and Title
Google Scholar: Author Only Title Only Author and Title

Arnesen T, Van Damme P, Polevoda B, Helsens K, Evjenth R, Colaert N, Varhaug JE, Vandekerckhove J, Lillehaug JR, Sherman F, Gevaert K (2009b) Proteomics analyses reveal the evolutionary conservation and divergence of N-terminal acetyltransferases from yeast and humans. Proc Natl Acad Sci U S A 106: 8157-8162

Pubmed: Author and Title
Google Scholar: Author Only Title Only Author and Title

Bernal-Perez LF, Prokai L, Ryu Y (2012) Selective N-terminal fluorescent labeling of proteins using 4-chloro-7-nitrobenzofurazan: A method to distinguish protein N-terminal acetylation. Analytical Biochemistry 428: 13-15

Pubmed: Author and Title
Google Scholar: Author Only Title Only Author and Title

Bienvenut WV, Giglione C, Meinnel T (2017a) SILProNAQ: A Convenient Approach for Proteome-Wide Analysis of Protein N-Termini and N-Terminal Acetylation Quantitation. Methods Mol Biol 1574: 17-34

Pubmed: Author and Title
Google Scholar: Author Only Title Only Author and Title

Bienvenut WV, Scarpelli JP, Dumestier J, Meinnel T, Giglione C (2017b) EnCOUNTer: a parsing tool to uncover the mature N-terminus of organelle-targeted proteins in complex samples. BMC Bioinformatics 18: 182

Pubmed: Author and Title
Google Scholar: Author Only Title Only Author and Title

Bienvenut WV, Sumpton D, Martinez A, Lilla S, Espagne C, Meinnel T, Giglione C (2012) Comparative Large Scale Characterization of Plant versus Mammal Proteins Reveals Similar and Idiosyncratic N-α-Acetylation Features. Molecular & Cellular Proteomics 11: M111.015131
Pubmed: Author and Title
Google Scholar: Author Only Title Only Author and Title

Blum H, Beier H, Gross HJ (1987) Improved silver staining of plant proteins, RNA and DNA in polyacrylamide gels. Electrophoresis 8: 93-99
Pubmed: Author and Title
Google Scholar: Author Only Title Only Author and Title

Bradford MM (1976) A rapid and sensitive method for the quantitation of microgram quantities of protein utilizing the principle of protein-dye binding. Anal Biochem 72: 248-254
Pubmed: Author and Title
Google Scholar: Author Only Title Only Author and Title

Caesar R, Blomberg A (2004) The stress-induced Tfs1p requires NatB-mediated acetylation to inhibit carboxypeptidase Y and to regulate the protein kinase A pathway. J Biol Chem 279: 38532-38543
Pubmed: Author and Title
Google Scholar: Author Only Title Only Author and Title

Caesar R, Warringer J, Blomberg A (2006) Physiological importance and identification of novel targets for the N-terminal acetyltransferase NatB. Eukaryot Cell 5: 368-378
Pubmed: Author and Title
Google Scholar: Author Only Title Only Author and Title

Casey JP, Støve SI, McGorrian C, Galvin J, Blenski M, Dunne A, Ennis S, Brett F, King MD, Arnesen T, Lynch SA (2015) NAA10 mutation causing a novel intellectual disability syndrome with Long QT due to N-terminal acetyltransferase impairment. Scientific Reports 5: 16022
Pubmed: Author and Title
Google Scholar: Author Only Title Only Author and Title

Chen Z, Zhao P-X, Miao Z-Q, Qi G-F, Wang Z, Yuan Y, Ahmad N, Cao M-J, Hell R, Wirtz M, Xiang C-B (2019) SULTR3s Function in Chloroplast Sulfate Uptake and Affect ABA Biosynthesis and the Stress Response. Plant Physiol 180: 593-604
Pubmed: Author and Title
Google Scholar: Author Only Title Only Author and Title

Czechowski T, Stitt M, Altmann T, Udvardi MK, Scheible WR (2005) Genome-wide identification and testing of superior reference genes for transcript normalization in Arabidopsis. Plant Physiol 139: 5-17
Pubmed: Author and Title
Google Scholar: Author Only Title Only Author and Title

Dinh TV, Bienvenut WV, Linster E, Feldman-Salit A, Jung VA, Meinnel T, Hell R, Giglione C, Wirtz M (2015) Molecular identification and functional characterization of the first Na-acetyltransferase in plastids by global acetylome profiling. Proteomics 15: 2426-2435
Pubmed: Author and Title
Google Scholar: Author Only Title Only Author and Title

Drazic A, Aksnes H, Marie M, Boczkowska M, Varland S, Timmerman E, Foyn H, Glomnes N, Rebowski G, Impens F, Gevaert K, Dominguez R, Arnesen T (2018) NAA80 is actin's N-terminal acetyltransferase and regulates cytoskeleton assembly and cell motility. Proc Natl Acad Sci U S A
Pubmed: Author and Title
Google Scholar: Author Only Title Only Author and Title

Dupree P, Sherrier DJ (1998) The plant Golgi apparatus. Biochim Biophys Acta 1404: 259-270
Pubmed: Author and Title
Google Scholar: Author Only Title Only Author and Title

Falb M, Aivaliotis M, Garcia-Rizo C, Bisle B, Tebbe A, Klein C, Konstantinidis K, Siedler F, Pfeiffer F, Oesterhelt D (2006) Archaeal N-terminal protein maturation commonly involves N-terminal acetylation: a large-scale proteomics survey. J Mol Biol 362: 915-924
Pubmed: Author and Title
Google Scholar: Author Only Title Only Author and Title

Ferrandez-Ayela A, Micol-Ponce R, Sanchez-García AB, Alonso-Peral MM, Micol JL, Ponce MR (2013) Mutation of an Arabidopsis NatB N-Alpha-Terminal Acetylation Complex Component Causes Pleiotropic Developmental Defects. PLoS ONE 8: e80697, 80691-80611
Pubmed: Author and Title
Google Scholar: Author Only Title Only Author and Title

Frottin F, Martinez A, Peynot P, Mitra S, Holz RC, Giglione C, Meinnel T (2006) The proteomics of N-terminal methionine cleavage. Mol Cell Proteomics 5: 2336-2349
Pubmed: Author and Title
Google Scholar: Author Only Title Only Author and Title

Giglione C, Fieulaine S, Meinnel T (2015) N-terminal protein modifications: Bringing back into play the ribosome. Biochimie
Pubmed: Author and Title
Google Scholar: Author Only Title Only Author and Title

Heeg C, Kruse C, Jost R, Gutensohn M, Ruppert T, Wirtz M, Hell R (2008) Analysis of the Arabidopsis O-acetylserine(thiol)lyase gene family demonstrates compartment-specific differences in the regulation of cysteine synthesis. Plant Cell 20: 168-185
Pubmed: Author and Title
Google Scholar: Author Only Title Only Author and Title

Helbig AO, Rosati S, Pijnappel PW, van Breukelen B, Timmers MH, Mohammed S, Slijper M, Heck AJ (2010) Perturbation of the yeast N-acetyltransferase NatB induces elevation of protein phosphorylation levels. BMC Genomics 11: 685
Pubmed: Author and Title
Google Scholar: Author Only Title Only Author and Title

Hong H, Cai Y, Zhang S, Ding H, Wang H, Han A (2017) Molecular Basis of Substrate Specific Acetylation by N-Terminal Acetyltransferase NatB. Structure 25: 641-649 e643
Pubmed: Author and Title
Google Scholar: Author Only Title Only Author and Title

Huang da W, Sherman BT, Lempicki RA (2009a) Bioinformatics enrichment tools: paths toward the comprehensive functional analysis of large gene lists. Nucleic Acids Res 37: 1-13
Pubmed: Author and Title
Google Scholar: Author Only Title Only Author and Title

Huang da W, Sherman BT, Lempicki RA (2009b) Systematic and integrative analysis of large gene lists using DAVID bioinformatics resources. Nat Protoc 4: 44-57
Pubmed: Author and Title
Google Scholar: Author Only Title Only Author and Title

Kaundal R, Saini R, Zhao PX (2010) Combining Machine Learning and Homology-Based Approaches to Accurately Predict Subcellular Localization in Arabidopsis. Plant Physiology 154: 36-54
Pubmed: Author and Title
Google Scholar: Author Only Title Only Author and Title

Linster E, Stephan I, Bienvenut WV, Maple-Grodem J, Myklebust LM, Huber M, Reichelt M, Sticht C, Geir Moller S, Meinnel T, Arnesen T, Giglione C, Hell R, Wirtz M (2015) Downregulation of N-terminal acetylation triggers ABA-mediated drought responses in Arabidopsis. Nat Commun 6: 7640
Pubmed: Author and Title
Google Scholar: Author Only Title Only Author and Title

Linster E, Wirtz M (2018) N-terminal acetylation: an essential protein modification emerges as an important regulator of stress responses. J Exp Bot 69: 4555-4568
Pubmed: Author and Title
Google Scholar: Author Only Title Only Author and Title

Nguyen KT, Kim JM, Park SE, Hwang CS (2019) N-terminal methionine excision of proteins creates tertiary destabilizing N-degrons of the Arg/N-end rule pathway. J Biol Chem 294: 4464-4476
Pubmed: Author and Title
Google Scholar: Author Only Title Only Author and Title

Nilsson OB, Hedman R, Marino J, Wickles S, Bischoff L, Johansson M, Muller-Lucks A, Trovato F, Puglisi JD, O'Brien EP, Beckmann R, von Heijne G (2015) Cotranslational Protein Folding inside the Ribosome Exit Tunnel. Cell Rep 12: 1533-1540
Pubmed: Author and Title
Google Scholar: Author Only Title Only Author and Title

Noji M, Inoue K, Kimura N, Gouda A, Saito K (1998) Isoform-dependent differences in feedback regulation and subcellular localization of serine acetyltransferase involved in cysteine biosynthesis from Arabidopsis thaliana. J Biol Chem 273: 32739-32745
Pubmed: Author and Title
Google Scholar: Author Only Title Only Author and Title

Pesaresi P, Gardner NA, Masiero S, Dietzmann A, Eichacker L, Wickner R, Salamini F, Leister D (2003) Cytoplasmic N-terminal protein acetylation is required for efficient photosynthesis in Arabidopsis. Plant Cell 15: 1817-1832
Pubmed: Author and Title
Google Scholar: Author Only Title Only Author and Title

Pierre M, Traverso JA, Boisson B, Domenichini S, Bouchez D, Giglione C, Meinnel T (2007) N-myristoylation regulates the SnRK1 pathway in Arabidopsis. Plant Cell 19: 2804-2821
Pubmed: Author and Title
Google Scholar: Author Only Title Only Author and Title

Polevoda B, Arnesen T, Sherman F (2009) A synopsis of eukaryotic Nalpha-terminal acetyltransferases: nomenclature, subunits and substrates. BMC Proc 3 Suppl 6: S2
Pubmed: Author and Title
Google Scholar: Author Only Title Only Author and Title

Polevoda B, Brown S, Cardillo TS, Rigby S, Sherman F (2008) Yeast N(alpha)-terminal acetyltransferases are associated with ribosomes. J Cell Biochem 103: 492-508

Pubmed: Author and Title
Google Scholar: Author Only Title Only Author and Title

Polevoda B, Cardillo TS, Doyle TC, Bedi GS, Sherman F (2003) Nat3p and Mdm20p are required for function of yeast NatB Nalpha-terminal acetyltransferase and of actin and tropomyosin. J Biol Chem 278: 30686-30697
Pubmed: Author and Title
Google Scholar: Author Only Title Only Author and Title

Polevoda B, Sherman F (2003) N-terminal acetyltransferases and sequence requirements for N-terminal acetylation of eukaryotic proteins. J Mol Biol 325: 595-622
Pubmed: Author and Title
Google Scholar: Author Only Title Only Author and Title

Ree R, Myklebust LM, Thiel P, Foyn H, Fladmark KE, Arnesen T (2015) The N-terminal acetyltransferase Naa10 is essential for zebrafish development. Biosci Rep 35
Pubmed: Author and Title
Google Scholar: Author Only Title Only Author and Title

Reid DW, Nicchitta CV (2015) Diversity and selectivity in mRNA translation on the endoplasmic reticulum. Nature reviews. Molecular cell biology 16: 221-231
Pubmed: Author and Title
Google Scholar: Author Only Title Only Author and Title

Rosso MG, Li Y, Strizhov N, Reiss B, Dekker K, Weisshaar B (2003) An Arabidopsis thaliana T-DNA mutagenized population (GABI-Kat) for flanking sequence tag-based reverse genetics. Plant Mol Biol 53: 247-259
Pubmed: Author and Title
Google Scholar: Author Only Title Only Author and Title

Sessions A, Burke E, Presting G, Aux G, McElver J, Patton D, Dietrich B, Ho P, Bacwaden J, Ko C, Clarke JD, Cotton D, Bullis D, Snell J, Miguel T, Hutchison D, Kimmerly B, Mitzel T, Katagiri F, Glazebrook J, Law M, Goff SA (2002) A high-throughput Arabidopsis reverse genetics system. Plant Cell 14: 2985-2994
Pubmed: Author and Title
Google Scholar: Author Only Title Only Author and Title

Singer JM, Shaw JM (2003) Mdm20 protein functions with Nat3 protein to acetylate Tpm1 protein and regulate tropomyosin-actin interactions in budding yeast. Proc Natl Acad Sci U S A 100: 7644-7649
Pubmed: Author and Title
Google Scholar: Author Only Title Only Author and Title

Starheim KK, Arnesen T, Gromyko D, Ryningen A, Varhaug JE, Lillehaug JR (2008) Identification of the human N(alpha)-acetyltransferase complex B (hNatB): a complex important for cell-cycle progression. Biochem J 415: 325-331
Pubmed: Author and Title
Google Scholar: Author Only Title Only Author and Title

Van Damme P, Lasa M, Polevoda B, Gazquez C, Elosegui-Artola A, Kim DS, De Juan-Pardo E, Demeyer K, Hole K, Larrea E, Timmerman E, Prieto J, Arnesen T, Sherman F, Gevaert K, Aldabe R (2012) N-terminal acetylome analyses and functional insights of the N-terminal acetyltransferase NatB. Proc Natl Acad Sci U S A 109: 12449-12454
Pubmed: Author and Title
Google Scholar: Author Only Title Only Author and Title

Xu F, Huang Y, Li L, Gannon P, Linster E, Huber M, Kapos P, Bienvenut W, Polevoda B, Meinnel T, Hell R, Giglione C, Zhang Y, Wirtz M, Chen S, Li X (2015) Two N-terminal acetyltransferases antagonistically regulate the stability of a nod-like receptor in Arabidopsis. Plant Cell 27: 1547-1562
Pubmed: Author and Title
Google Scholar: Author Only Title Only Author and Title